Neural Phenotype of Obesity: A Population-Based Approach

THESIS

Presented in Partial Fulfillment of the Requirements for the Degree Master of Science in the Graduate School of The Ohio State University

By

Samantha Jacobs Chavez, A.B.

Graduate Program in Public Health

The Ohio State University

2017

Master's Examination Committee:

Sarah E. Anderson, Advisor

Amy K. Ferketich

Abigail B. Shoben

Dylan D. Wagner

Abstract

Introduction:

Exploring individual differences in brain structure may augment our understanding of the social determinants of health. This thesis explores the relationship between obesity and white matter microstructural differences in a representative sample of adults from Rockland County, New York, to determine how neural phenotypes may work in concert with psychological traits (e.g., impulsivity) and sociodemographic factors to give rise to health outcomes. We hypothesize that the integrity of a "reward pathway" connecting the nucleus accumbens (NAcc) to the orbitofrontal cortex (OFC) will be positively associated with the odds of obesity, while the integrity of an "inhibitory pathway" connecting the OFC to the inferior frontal gyrus (IFG) will be negatively associated with the odds of obesity.

Study Population:

We used data from a sample of 275 adults (aged 18-85 years) enrolled in the enhanced Nathan Kline Institute-Rockland Sample (NKI-RS).

Methods and Materials:

Imaging data were acquired on a Siemens Magnetom TrioTim 3.0 Tesla MRI scanner. NAcc parcellations were made by applying FSL's FIRST to each subject's T1-

weighted MP-RAGE sequence. OFC masks were derived using the reverse inference feature of Neurosynth's automated meta-analysis. Three white matter tracts were defined: two via probabilistic tractography maps generated with FSL's BEDPOSTx single-mask seeding procedure with 5000 probabilistic streamlines originating from each NAcc voxel and passing through the OFC, and one pre-defined tract based on prior work connecting the left OFC and the left IFG. Structural integrity of each white matter pathway was defined as each subject's mean fractional anisotropy (FA) within each non-overlapping tract. Body mass index (BMI) was computed based on weight in kilograms divided by height in meters squared. We defined obesity as a BMI at or exceeding 30 kg/m^2.

A predictive modeling approach was used to build a logistic regression model in a training dataset, with an effort to maximize the sensitivity and specificity with which we could predict the log-odds of obesity in a hold-out sample. The cut point corresponding to the probability of obesity that best maximized sensitivity and specificity in the training dataset was chosen to test the efficacy of the model's ability to predict the obesity status of participants in the holdout sample.

Results:

The prevalence of obesity in the training dataset was 25.1%; the prevalence of obesity in the validation dataset was 39.2%. Based on the training data, we observe a strong positive association between impulsivity and the odds of obesity, such that a 10-unit increase on the UPPS-P Impulsive Behavior Scale was associated with a 38% increase in the odds of obesity. Mean FA in the tract connecting the left OFC to the left

NAcc, which we operationalize as a "reward pathway", is also positively associated with the odds of obesity, such that a 0.01-unit increase in mean FA in this tract predicts a 54% increase in the odds of obesity. Conversely, mean FA in the tract connecting the left OFC to the left IFG, which we operationalize as an "inhibitory pathway", is inversely associated with the odds of obesity; for each 0.01-unit increase in mean FA within this pathway, we observe a 39% decrease in the odds of obesity.

Using a 0.27 probability cutoff for predicting obesity, 63.5% of participants in the holdout sample were correctly classified with respect to obesity status. Predictions in the holdout sample corresponded to sensitivity of 72.4% and specificity of 57.8%.

Discussion:

Our results suggest that there may be a neural phenotype of current obesity, such that, for two individuals with comparable microstructural integrity in a "reward pathway", differences in the white matter coherence in an "inhibitory pathway" can meaningfully predict differences in obesity status. Moreover, by using a representative sample of Rockland County adults, we can quantify the degree to which these pathways may be more or less influential as a function of age, sex, and parental socioeconomic status. Future work to determine whether individual differences in the integrity of these pathways are a cause or consequence of obesity is needed. Additionally, it may be of interest to explore whether differences in these pathways uniquely predict obesity or if, instead, they can be better conceived of as a domain-general risk factor for health status related to impulsivity (e.g., predicting the odds of being a current smoker).

Vita

2006 …… Coursework, Harvard University

2007 …… Marywood-Palm Valley School

2009 to 2012 ……... Undergraduate Research Assistant, Department of Government, Dartmouth College

2009 to 2012 ……... Undergraduate Research Assistant, Department of Psychological and Brain Sciences, Dartmouth College

2012 ……..... A.B. Psychology and Government, Dartmouth College

2012 to 2016 ……... Lab Manager, Department of Psychological and Brain Sciences, Dartmouth College

2015 to present ……..... Graduate Research Assistant, Division of Epidemiology, College of Public Health, The Ohio State University

Publications

Kim, M.J., Brown, A.C., Mattek, A.M., Chavez, S.J., Taylor, J.M., Palmer, A.L., Wu, Y-C., & Whalen, P.J. (2016) The inverse relationship between the microstructural variability of amygdala-prefrontal pathways and trait anxiety is moderated by sex. *Frontiers in Systems Neuroscience, 10*, 93.

Whalen, P.J., Neta, M., Kim, M.J., Mattek, A.M., Davis, F.C., Taylor, J.M., & Chavez, S. (2017) Neural and behavioral responses to ambiguous facial expressions of emotion. In: Fernandez Dols, J.M. & Russell, J.A. (Eds.) *The Science of Facial Expression*. New York: Oxford University Press.

Fields of Study

Major Field: Public Health

Table of Contents

Abstract …….. ii

Vita …… v

List of Tables …… x

List of Figures ……... xi

Introduction: Population Neuroscience ……..... 1

Background 4

Obesity Epidemiology …….. 4

Impulsivity and its Relationship to Obesity …….. 5

Impulsivity and its Relationship to the Brain ……... 6

Sleep Duration and its Relationship to Obesity …… 8

Sleep Duration and its Relationship to the Brain …….. 9

Neural Correlates of Sociodemographic Factors ……. 10

Neuroarchitectural Changes Over the Lifespan ……... 10

Neuroarchitectural Differences by Socioeconomic Status …….. 12

Neuroarchitectural Differences by Race and Ethnicity ……... 14

Neuroarchitectural Variability and its Relationship to Impulsivity ……..... 15

Research Question ……... 16

Hypotheses ……... 17

Methods …… 18

Sample and Study Design …… 18

Participant Data Collection Schedule …….. 21

Obtaining Participant Data ……... 22

Physical and Demographic Measures …….. 24

Behavioral Measures ……..... 27

Image Acquisition …… 28

Defining Seed, Waypoint, and Exclusion Masks ……. 29

Preprocessing and Probabilistic Tractography ……. 31

Analytic Strategy ……. 36

Results …….. 40

Model Building …… 43

Interpretation of Model Coefficients ……... 46

Model Fit, Adequacy and Discrimination …… 50

Model Diagnostics ……... 52

Model Validation …… 58

Importance of Taking a Multi-Disciplinary Approach …… 59

Discussion …… 61

Strengths and Limitations …… 63

Future Directions …… 65

Public Health Relevance …….. 66

Conclusions …….. 67

References …… 68

Appendix: UPPS-P Impulsive Behavior Scale …… 78

List of Tables

Table 1. Generalizability of Rockland Sample …… 20

Table 2. Descriptive Statistics (Overall and by Obesity Status and Impulsivity) ...…… 41

Table 3. Univariable Analyses ……. 43

Table 4. Final Model Parameters ……. 46

Table 5. Correlation Matrix for Final Model Covariates ……. 47

Table 6. Sensitivity, Specificity, and Classification Accuracy as a function of Probability Cutoffs ……. 51

Table 7. Effect of Removing Extreme Covariate Patterns ……... 56

Table 8. Classification Accuracy: Model Building vs. Model Validation Datasets …… 59

List of Figures

Figure 1. Warping Masks from Standard to Native Space …….. 31

Figure 2. Process for Extracting Mean Fractional Anisotropy …… 34

Figure 3. Addressing the Issue of Overlapping White Matter Tracts …….. 35

Figure 4. Distribution of BMI in the Model Building Dataset …… 40

Figure 5. Correlation Between Integrity of "Inhibitory" and "Reward" Pathways ……. 48

Figure 6. Predicted Probability of Obesity as a Function of Age for Hypothetical Male Subjects with All Other Covariates Held Constant ……. 49

Figure 7. Final Model: Graph of Sensitivity and Specificity vs. Probability Cutoffs …. 50

Figure 8. Final Model: Receiver Operating Characteristic Curve ……... 52

Figure 9. Model Diagnostics: Identifying Covariate Patterns with High Leverage …… 53

Figure 10. Model Diagnostics: Identifying Covariate Patterns with High Residuals ….. 54

Figure 11. Model Diagnostics: Identifying Covariate Patterns with High Influence ….. 55

Introduction: Population Neuroscience

Population neuroscience is an emerging discipline that couples detailed genetic and neural information at the individual level with data collection procedures on a grand scale that use population-based sampling methods (Paus, 2013). The human neurosciences have made great strides in recent years toward explicating brain-behavior relationships and their psychosocial correlates [e.g., from social neuroscience see (Cacioppo, Berntson, Sheridan, & McClintock, 2000) & (Steinberg, 2008); from decision neuroscience, see (Coultee & Huettel, 2012); for a general review, see (Berkman & Falk, 2013)]. However, much of this work has emphasized the individual and his/her micro-level neuroarchitecture [e.g., see (Hariri, 2009)]. Very often, study recruitment takes the form of a convenience sample, leading to an overrepresentation of young, educated, liberal, Caucasian persons (Henrich, Heine, & Norenzayan, 2010), thereby failing to account for any differences at the neural level as a function of membership in other sociodemographic groups. There has been a tendency to prioritize the individual over his/her social environment, and as such, neuroscientists have only recently begun to characterize the "representative brain" and how it interacts within the more macro-level facets of its social milieu (Falk, et al., 2013). How is our current knowledge qualified by racial-ethnic identity, socioeconomic status, geographic locale, and educational attainment? And can one really use a neuroscientific approach to address public health

outcomes without knowing whether the extant literature generalizes to the larger population of interest?

Neuroscience has a lot to offer the public health discourse, by defining new neural risk factors related to decision making and impulse regulation, which may aid or impede efforts to maintain healthy behaviors. However, future research would benefit from taking an integrated, interdisciplinary approach that combines detailed neural phenotyping with population-based sampling methods. As it stands, many pieces of the puzzle (individual differences in geneotypes, neural phenotypes, personality traits, behavioral tendencies, socioeconomic and demographic factors) have been collected, but they are, for the most part, not yet assembled into a coherent picture that addresses how each puzzle piece comes together to influence health status. It is not enough to ask what genetic predispositions shape the neural landscape [e.g., see (Hibar, et al., 2015)]. It is not enough to ask which personality traits are associated with the tendency to behave in one way or another [e.g., see (Salgado, 2002)]. It is not enough to ask how our social networks give rise to healthy psychological functioning [e.g., see (Uchino, 2006)]. And it is not enough to ask which demographic risk factors affect our long-term health [e.g., see (Lantz, et al., 1998)]. None of these questions can give us a complete picture. It is far more likely that personality traits, behavioral dispositions, and societal and environmental exposures coalesce and interact to give rise to health outcomes, mediated by neural processes. By widening the scope of an epidemiological approach to include the "black box" of the brain bases of health behavior, we can gain important insights into the mechanisms that give rise to disease (Paus, 2013). Moreover, we can exploit knowledge

gained from this new population neuroscience perspective to further public health goals (e.g., reducing obesity, curtailing substance abuse, alleviating symptoms of anxiety and depression, etc.). Population neuroscience may better equip us to predict negative health outcomes before they manifest and to develop more targeted treatments that account for the inter-individual variability of disease at the molecular, neural, individual, and societal levels.

Background

Obesity Epidemiology

The prevalence of overweight and obesity among adults in the United States exceeds two-thirds of the population [68.5% overweight or obese (Ogden, Carroll, Kit, & Flegal, 2014); 35.2% obesity among men, 40.5% obesity among women (Flegal, Kruszon-Moran, Carroll, Fryar, & Ogden, 2016)]. Among Hispanics (38.8% males; 46.6% females) and non-Hispanic black females (57.2%), prevalence of obesity is particularly high (Flegal, Kruszon-Moran, Carroll, Fryar, & Ogden, 2016). Overweight status can be linked to cardiovascular disease (Klein, et al., 2004) and risk of coronary heart disease (Baker, Olsen, & Sorensen, 2007), increased risk of stroke, diabetes, certain cancers [e.g., see (Calle, Rodriguez, Walker-Thurmond, & Thun, 2003) and (Guh, et al., 2009)], and a host of assaults on psychological health, including comorbid anxious and depressive symptomatology and low self-esteem [e.g., see (Strauss & Pollack, 2003), (Puhl & Heuer, 2009), and (Kottke, Wu, & Hoffman, 2003)], to name just a few negative health consequences. The social ramifications associated with overweight are equally impressive: lower household income, fewer completed years of education, greater difficulty finding a romantic partner, employment discrimination (Haas, et al., 2003), and undesirable associations in the public consciousness [e.g., the notion that fat people are dumb, lazy, unhygienic, and dishonest; (Puhl & Heuer, 2009)]. And finally, the

economic impact of obesity-related conditions accounts for more than 20% of all health care expenditures in the United States, exceeding $275 billion annually (Spieker & Pyzocha, 2016).

Impulsivity and its Relationship to Obesity

Our capacity to regulate impulsive urges is instrumental in the development and maintenance of healthy food behaviors and goals (Mobbs, Crepin, Thiery, Golay, & Van der Linden, 2010). Impulsive behavior may be indicative of a deficit in the capacity to quickly inhibit responses (Logan, Schachar, & Tannock, 1997). Impulsive persons tend to engage in delayed discounting (whereby rewards lose value as their attainment becomes more distal) and sensation seeking (a personality trait characterized by risk-taking in an effort to experience and feel extremes); they have trouble waiting and often fail to consider long-term consequences (Ainslie, 1975). Higher self-reported impulsivity is associated with increased risk of alcohol and drug addiction, attention-deficit/hyperactivity disorder, conduct disorder (Johnson, Turner, & Iwata, 2003), problem gambling (Lawrence, Luty, Bogdan, Sahakian, & Clark, 2009), risk taking and unintentional injury (Ryb, Dischinger, Kufera, & Read, 2006), and overindulgence in appetizing foods (Nederkoorn, Braet, Van Eijs, Tanghe, & Jansen, 2006), suggesting that high levels of impulsivity may be a general indicator of vulnerability (Verdejo-Garcia, Lawrence, & Clark, 2008),.

The ability to delay gratification (i.e., the capacity to wait for a reward) can be conceptualized as a component of impulse control (Mischel, 1974). In a seminal series of experiments designed to probe delayed gratification mechanisms in preschoolers, Mischel and colleagues designed the "marshmallow task" (Mischel, Ebbesen, & Raskoff Zeiss, 1972). Participants were offered a desired snack (a marshmallow or pretzel) and told that the experimenter had to leave the room briefly. If the child could wait until the experimenter returned before eating the snack, then s/he would be rewarded with another snack. If the child was unable to exercise restraint, there would not be a second snack. More concretely, a child who waits gets two marshmallows, while a child who gives in to temptation gets only one marshmallow. Of particular interest, these studies revealed large individual differences in children's ability to exert self-control, and these differences not only persisted 10 years afterward, but also predicted academic performance and emotional stability into the adolescent years and beyond (Mischel, Shoda, & Rodriguez, 1989). In fact, ability to delay gratification at preschool-age is associated with body mass index three decades later (Schlam, Wilson, Shoda, Mischel, & Ayduk, 2013).

Impulsivity and its Relationship to the Brain

Before discussing impulsivity's neural substrates, it may be useful to introduce some neuroimaging methodology. Diffusion tensor imaging (DTI) is a method of indexing the microstructural properties of connections (white matter) between different

brain regions (grey matter). DTI can aid in probabilistically determining which structures are connected to one another and quantify the degree of coherence in these connections [e.g., see (Le Bihan, et al., 2001) and (Behrens, Berg, Jbabdi, Rushworth, & Woolrich, 2007)]. Fractional anisotropy (FA) is a commonly used DTI-derived measurement that reflects white matter fiber density and the width and myelination of axons (Emsell, Van Hecke, & Tournier, 2016). FA values represent a continuous scalar measurement (ranging from 0-1) of the integrity of white matter (Basser & Pierpaoli, 1996), such that higher FA values indicate more organized, healthier connections.

Recently, frontostriatal connectivity has been implicated in the trajectory of emergent delayed gratification abilities, such that white matter integrity, as measured via fractional anisotropy derived from diffusion tensor imaging, independently accounts for a portion of the variability in existing and future impulse control (Achterberg, Peper, van Duijvenvoorde, Mandl, & Crone, 2016). Of particular public health relevance, this research suggests that similar cytoarchitecture may underlie health behaviors related to impulsivity, like dietary intake. Frontostriatal development, thus, might clarify the relationship between self-regulatory control and the odds of obesity.

A recent review of white matter microstructural changes associated with obesity (Kullmann, Schweizer, Veit, Fritsche, & Preissl, 2015) implicates a complex pattern of reduced fractional anisotropy values in prefrontal regions important for inhibitory control and in the fornix and cingulum, well-known fiber bundles within the limbic system. Furthermore, an analysis of FA network clustering and strength within the putative neural

reward circuitry links fewer probabilistic streamlines (an indication of less anatomical wiring in a particular region) and lower microstructural integrity within the OFC and striatum (including the NAcc) to obesity status (Marques-Iturria, et al., 2015). Additionally, dorsomedial, dorsolateral, and ventrolateral prefrontal regions (dmPFC; dlPFC; vlPFC) have been reliably implicated in the down-regulation of craving for food and drugs of addiction, and most notably for the present research question, a functional dlPFC-striatal pathway may mediate successful regulation in the face of appetitive stimuli (Kober, et al., 2010). Finally, the integrity of a white matter tract connecting the left inferior frontal gyrus (lIFG), implicated in inhibitory processes (as well as language comprehension and speech production), to the orbitofrontal cortex has been linked to body fat percentage in dieters, such that higher tract coherence is associated with reduced body fat (Chen, Chavez, & Heatherton, 2016). If we could use this combined knowledge to predict risk for negative health outcomes associated with impulsivity and self-regulatory failure, we might be better able to allocate resources toward those who need it most, and to intervene earlier to curb disease. Analysis of neuroimaging data collected via population-based sampling methods may allow for better generalizability of the speculative relationships between brain structure and health behaviors.

Sleep Duration and its Relationship to Obesity

A recent meta-analysis of 36 population-based samples including over 600,000 participants aged 2-102 years suggests that short sleep duration increases the odds of

obesity (Cappuccio, et al., 2008). Children (2-17 years of age) who slept less than 10 hours per night had an 89% increased odds of obesity, as defined by a BMI exceeding the 95th percentile according to national or international growth charts (depending on the study population). Adults (18-102 years of age) who slept less than or equal to 5 hours per night had a 55% increased odds of obesity, as defined by a BMI meeting or exceeding 30 kg/m^2. Pooling across studies, the authors report that there is evidence of a linear association between sleep duration and BMI in adults, such that, for every 1 hour reduction in sleep duration, they observe a 0.35-unit increase in BMI. In contrast, others report that, while there may be an inverse linear association between sleep duration and BMI in children, this relationship does not hold across the life course; the relationship may be U-shaped in middle-aged persons (30-64 years old), and non-significant in older age [≥65 years old; (Grandner, Schopfer, Sands-Lincoln, Jackson, & Malhotra, 2015); also, see (Patel & Hu, 2008)]. Therefore, while most agree that sleep duration is associated with obesity, there is controversy over how this relationship may or may not change across the life course.

Sleep Duration and its Relationship to the Brain

There is some evidence that increased sleep duration may aid in increased synaptic reorganization and neurogenesis within the hippocampus during childhood [e.g., see (Taki & Kawashima, 2012)], which may have important implications for the role of sleep duration in memory reconsolidation and response inhibition. However, while this

relationship has been observed in children, there does not seem to be a relationship between hippocampal volume and sleep in adults (Winkelman, et al., 2010). Others have documented associations between sleep duration and regions of the brain implicated in reward-processing and cognitive control; in a population of adolescents, shorter sleep duration was associated with functional decoupling between the dorsolateral prefrontal cortex and the ventral striatum during a reward processing task (Telzer, Fuligni, Lieberman, & Galvan, 2013). Interestingly, this research group also conducted a longitudinal study investigating structural differences associated with sleep in adolescents; they find that sleep *variability*, not sleep *duration*, is associated with lower FA globally (Telzer, Goldenberg, Fuligini, Lieberman, & Galvan, 2015). Therefore, to the extent that sleep duration does impact neural structure, this impact may vary as a function of age. It is also possible that sleep duration may be a poor proxy for sleep quality's effect on the brain, and that sleep variability may be a more appropriate measure.

Neural Correlates of Sociodemographic Factors

Neuroarchitectural Changes Over the Lifespan

It has been well-established that changes in brain structure are evident across the lifespan. For example, in a sample of 176 subjects aged 7-87 years, grey matter density declined with age, and this decline was linear in brain regions that myelinate early (e.g., visual and limbic cortices), but nonlinear in brain regions that myelinate well into

adulthood [e.g., frontal and parietal cortices; (Sowell, Peterson, Thompson, Welcome, Henkenius, & Toga, 2003)]. With respect to white matter tract evolution, Lebel and colleagues show that, in a sample of 403 subjects aged 5-83 years, fractional anisotropy increases during childhood and adolescence, peaks in early adulthood (somewhere between 20-42 years of age), and then decreases (Lebel, Gee, Camicioli, Wieler, Martin, & Beaulieu, 2012). However, these trends are averages over the twelve largest white matter pathways; there is still considerable variability between the developmental trajectories of different pathways.

Age-related microstructural change does not occur uniformly throughout the brain; interestingly, FA in connections between frontal and temporal regions seems to peak later in life, while FA in connections between limbic regions tends to peak earlier in life. These findings have been replicated in independent samples [e.g., see (Kochunov, et al., 2012)]. Additionally, a recent review suggests that some age-related changes in later life affecting value-based decision making, driven by prefrontal and NAcc structural changes (Samanez-Larkin & Knutson, 2015), may be subject to individual differences in white matter coherence. This suggests that age may be an important predictor of health status related to reward-seeking behaviors. Studies attempting to characterize the effects of brain structure on health may, therefore, be best served by samples that utilize a lifespan approach.

Neuroarchitectural Differences by Socioeconomic Status

A considerable body of evidence documents the effects of socioeconomic status (SES) on brain morphometry (i.e., volume and surface area) during early development [e.g., see (Noble, Houston, Kan, & Sowell, 2012) and (Jednorog, et al., 2012)]. While these studies document volumetric differences associated with SES (e.g., in the amygdala and hippocampus), little is known about functional differences in neuroanatomy. A few studies document parental SES disparities in children's cognitive function during language processing tasks [e.g., (Noble, Wolmetz, Ochs, Farah, & McCandliss, 2006) and (Raizada, Richards, Meltzoff, & Kuhl, 2008)]. Importantly for this thesis, Raizada and colleagues found that performance on a rhyming task at five years of age was associated with recruitment of the left inferior frontal gyrus (lIFG; an area implicated in language processing and executive function), and that this relationship was moderated by SES. Higher SES was associated with greater recruitment of lIFG, which was in turn associated with better cognitive performance. Given that the lIFG has also been implicated in cue-reactivity to appetizing foods in chronic dieters, and that reduced integrity of a white matter pathway between the lIFG and the OFC was linked to having a greater body fat percentage in dieters (Chen, Chavez, & Heatherton, 2016), it may be especially important to see if these associations are qualified by different levels of SES.

Research has begun to investigate whether childhood SES impacts brain structure or function in adulthood [e.g., (Gianaros, et al., 2008)]. For example, Gianaros and colleagues find that adults with early socioeconomic disadvantage recruit the bilateral

amygdala (an area involved in emotional processing, saliency, and regulation) while viewing threatening facial expressions to a greater degree than participants who experienced relative socioeconomic advantage during childhood. Importantly, this relationship was not attenuated by participants' own social standing, suggesting that exposure to stressors related to the socioeconomic climate during childhood may imprint lasting change in the brain. Additionally, others (Gianaros, et al., 2011) have found that more years of parental education were associated with greater cortiostriatal connectivity (including regions of the bilateral orbitofrontal cortex and the left ventral striatum) during a monetary reward task in adulthood. Again, these results persisted even after controlling for participants' own educational attainment (which was not independently related to corticostriatal functioning).

Unfortunately, the literature pertaining to white matter microstructural correlates of socioeconomic disparity is especially sparse. There is some preliminary evidence (Gianaros, Marsland, Sheu, Erickson, & Verstynen, 2013) to suggest that global white matter integrity is positively associated with SES variables – including years of education, household income, and neighborhood-level SES – even after controlling for anxious and depressive symptoms and number of negative life events. Notably, the authors find that several health-related factors mediate the relationship between SES and white matter microstructure. For example, the authors find that the process by which lower SES yields reduced fractional anisotropy values happens through indirect paths of increased cigarette smoking and adiposity (as measured by waist circumference).

Neuroarchitectural Differences by Race and Ethnicity

Little is known about differences in white matter microstructural integrity across different racial-ethnic groups. In fact, one might argue about whether or not it is even appropriate to construe race or ethnicity as subject to biological variability (Winker, 2004) in brain structure or function. Few neuroimaging studies report the racial or ethnic composition of their samples, and only a handful of studies aim to systematically investigate differences in brain morphometry across racial-ethnic groups. I was only able to identify one study (Hsu, et al., 2016) that investigated racial differences in brain structure as they pertained to obesity. Hsu and colleagues found differences in the relationship between hippocampal volume and BMI across African Americans and European Americans with Type II diabetes, such that hippocampal *grey* matter volume and BMI were inversely correlated, but only among African Americans. In contrast, the authors found a significant inverse association between hippocampal *white* matter volume and waist circumference, irrespective of racial background. To the extent that obesity status is represented disparately in the brain across racial-ethnic groups, these differences may only be expressed in grey matter correlates. The present study is concerned exclusively with mean fractional anisotropy, which is a measure of white matter integrity. There is, to our knowledge, no literature to suggest any expected differences in white matter microstructure across racial-ethnic groups that cannot be explained by other socioeconomic or psychological factors.

Neuroarchitectural Variability and its Relationship to Impulsivity

The brain structures and connections subserving impulsive behavior and inhibitory control do not develop or degenerate uniformly within or between individuals, suggesting that there may be periods of neural plasticity in the capacity for impulse control [(Blakemore & Choudhury, 2006); (Vink, Kleerekooper, van den Wildenberg, & Kahn, 2015); (Olson, et al., 2009); (Samanez-Larkin, Levens, Perry, Dougherty, & Knutson, 2012)]. The degree to which subcortical regions involved with affect-laden associative learning (e.g., nucleus accumbens; NAcc) develop faster than cortical regions linked to cue-reactivity (Kringelbach, 2005) and self-regulation [(Heatherton & Wagner, 2011); e.g., orbitofrontal and dorsolateral prefrontal cortices, respectively] represents a developmental mismatch of the putative "self-control" circuitry of the brain [(Mills, Goddings, Clasen, Giedd, & Blakemore, 2014); (Somerville, Jones, & Casey, 2010)].

Research Question

Social structures and contextual factors may influence self-regulatory behavior; disadvantaged sociodemographic groups may be predisposed to favor immediate rewards over long-term consequences after repeated exposure to environmental stressors that require constant vigilance (Williams & Collins, 2001). Additionally, there are known associations between self-control deficits and dopamine receptor dysfunction, which may be indicative of reduced striatocortical integrity (Tomasi & Volkow, 2013). Obesity has been reliably implicated in particular neural substrates (e.g., striatum and prefrontal cortex) and with impulsive personality traits and sociodemographic risk factors (e.g., minority race, older age, etc.). By taking a multi-perspective approach that combines epidemiology, psychology, and neuroscience, we can begin to investigate the biological mechanisms of self-regulatory failure in an effort to elucidate their mediating role in the social determinants of health and disease. A focal point of this thesis strives to conduct a social neuroscience analysis with data that were collected using population-based sampling methods (i.e., NKI-RS), both to increase our confidence that inferences drawn from our neuroimaging analyses are generalizable, and to ensure that potential differences as a function of socioeconomic or demographic factors are not overlooked.

Hypotheses

We will use probabilistic tractography from diffusion imaging data collected from a representative sample of residents of Rockland County, New York (see *Sample and Study Design* below), to identify two white matter tracts that have been reliability implicated in disinhibition (NAcc ←→ OFC) and self-control (OFC ←→ lIFG) processes, respectively. We hypothesize that the integrity of the white matter microstructure in these neural pathways will clarify the relationship between impulsive tendencies and risk of obesity, and that these associations will be moderated by socioeconomic status. In particular, we predict that mean fractional anisotropy (FA) in a white matter pathway connecting the nucleus accumbens and the orbitofrontal cortex will be positively associated with the odds of obesity. Conversely, we predict that mean FA in a tract connecting the orbitofrontal cortex to the left inferior frontal gyrus will be inversely associated with the odds of obesity. Additionally, we expect that these relationships will be qualified by self-reported impulsivity, socioeconomic status during childhood, and participant age and typical nighttime sleep duration. Participant sex and racial-ethnic background will also be examined, though we have no directional hypotheses regarding these variables. We anticipate a positive association between impulsivity and the odds of obesity, a negative association between parental socioeconomic status and the odds of obesity, and nonlinear associations between both age and nighttime sleep duration, respectively, and the odds of obesity.

Methods

Sample and Study Design

We analyzed data from the enhanced Nathan Kline Institute-Rockland Sample (NKI-RS), which is designed to detect and track psychiatric illness across the lifespan (Nooner, et al., 2012). With the goal of using behavioral, neural, and genetic biomarkers to identify departures from normative psychosocial health, data are being collected across multiple modalities [including: diagnostic, behavioral, and cognitive assessments; resting state functional magnetic resonance imaging, diffusion tensor imaging, real-time neurofeedback sequences; blood (e.g., glucose and lipid panels) and urinalysis, etc.]. The Cross-Sectional Lifespan Connectomics Study (arm of NKI-RS used for analyses in this thesis) aims to build on the success of the 1000 Functional Connectomes Project with the additional goal of creating a large-scale lifespan sample that is representative of Rockland County, with oversampling during early development and older age, to be shared prospectively on a weekly basis. Target enrollment by age is as follows: 150 children aged 6-10 years, 150 adolescents and young adults aged 11-20 years, 100 adults aged 21-30 years, 75 adults aged 31-40 years, 100 adults aged 41-50 years, 125 adults aged 51-60 years, 150 adults aged 61-70 years, and 150 adults aged 71-85 years.

Sampling is community-ascertained, with a concerted emphasis on avoiding recruitment biases inherent to many brain-imaging studies, which tend to use

convenience samples. NKI-RS participant enrollment has been carefully controlled to ensure proportionate representation of each zip-code within Rockland County, New York, USA with respect to racial-ethnic background and socioeconomic status. Sampled participants are aged 6-85 years. Children younger than 6 years and older than 85 years are excluded due to practical considerations [i.e., young children have difficulty limiting movement during scanning, resulting in an excessive amount of unusable data; persons over the age of 85 are disproportionately likely to suffer from chronic illnesses that may impede eligibility (e.g., having a pacemaker)]. While participant recruitment is ongoing, current sample demographics (as of Sept. 2016) suggest that the 2014 U.S. census estimates of racial and ethnic diversity within Rockland County are well-captured. Moreover, socioeconomic and racial-ethnic characteristics of Rockland County are largely representative of the greater United States population (U.S. Census Bureau, 2015), which may aid in the generalizability of conclusions drawn from NKI-RS data (see Table 1). Every effort is being made to achieve full coverage of the target population; so far, study brochures were distributed to more than 100,000 households in Rockland County and advertisements have been placed on social networking sites and posted through free media sources (e.g., in shopping malls, community centers, schools, etc.). Exclusion criteria were minimal, and related to conditions affecting safety in an MRI environment (e.g., no ferrous metal in the body and no history of claustrophobia), age under 6 years or over 85 years, and primary residence outside of Rockland County, New York. The following inclusion criteria were applied for analyses in this thesis: 1) 18-85 years of age; 2) data release available in BIDS format (resulting in the use of Data

Releases 4 through 8 only); 3) available data on height and weight at study enrollment; 4) a completed high-resolution anatomical scan; and 5) a completed diffusion imaging scan that did not exhibit excessive head motion (see section on **Preprocessing and Probabilistic Tractography** for details).

People Facts (Census 2015)	United States	Rockland County	Nathan Kline Institute – Rockland Sample	Sample Used for Thesis
Population (n)	321 418 820	326 037	1 059	279
Age				
Persons under 5 years, % of population	6.2%	7.5%	0.0%*	0.0%
Persons under 18 years	22.9%	27.7%	24.8%	0.0%
Persons 65 years and over	14.9%	15.1%	15.1%	22.9%
Female persons	50.8%	51.0%	59.5%	73.1%
Race				
White	77.1%	77.5%	71.3%	75.3%
Black or African American	13.3%	13.2%	19.0%	15.8%
American Indian/Alaska Native	1.2%	0.5%	1.0%	0.7%
Asian	5.6%	6.7%	5.5%	3.2%
Native Hawaiian/Pacific Islander	0.2%	0.1%	0.5%	0.0%
Multiple races or Other Race reported	2.6%	1.9%	2.7%	3.9%
Hispanic or Latino	17.6%	17.4%	12.8%	10.8%
Language other than English spoken at home	20.9%	37.6%	22.3%	22.3%
High School graduates	86.3%	87.3%	99.1%	99.1%
Bachelor's degree or higher	29.3%	40.7%	53.7%	53.7%
Persons per household, 2010-2014	2.6	3.2	3.4	3.4
Median household income, 2010-2014	$53 482	$85 808	$50 000 to $75 000	$50 000 to $75 000
Per capita money income, 2010-2014	$28 555	$34 833	Not Available	Not Available
Persons below poverty level	13.5%	14.7%	≥9.0%	≥9.0%

Table 1. Generalizability of the Rockland Sample

Racial-ethnic and economic demographics of the United States (U.S. Census Bureau, 2015), Rockland County, New York, the Enhanced Nathan Kline Institute Rockland Sample (NKI-RS), and the subsample of NKI-RS used for this thesis.

The NKI-RS sample is comprised of four ongoing studies: 1) Cross-Sectional Lifespan Connectomics Study; 2) Longitudinal Developmental Connectomics Study; 3) Real-Time Neurofeedback; and 4) Adult Longitudinal Study. Though all of these studies have unique goals, enrollment is overlapping across studies, such that many participants enrolled in studies two through four were initially recruited for cross-sectional study one. For cases in which a participant was enrolled in multiple studies, only *baseline* demographic, physical, behavioral, and neural measures were used.

Participant Data Collection Schedule

While all participants had the opportunity to complete all questionnaires and imaging sequences relevant to this thesis, the order in which data were collected was not consistent across all participants. Participants enrolled prior to September 15, 2015 underwent a 2-day protocol in which physiological measures (including height and weight) were taken prior to breakfast, around 8:45AM on Schedule Day 1. Demographics, medical history, and several personality questionnaires were administered at 1:45PM on Schedule Day 1. For these participants, imaging was conducted on Schedule Day 2, beginning at 9:00AM, and behavioral measures related to eating, cognitive and executive functioning, risk taking and impulsivity, and affect (among others) were administered at 10:45AM on Schedule Day 2. For those enrolled on or after September 15, 2015, participants underwent a screening visit and a 1-day protocol. During the screening visit, demographic and physiological measures were obtained and

participants were sent an online assessment to be completed prior to the 1-day protocol. This online assessment consisted of questionnaires related to personality, eating, risk taking and impulsivity, and affect (among others). During the 1-day protocol, imaging was conducted shortly after breakfast at 9:00AM, medical history was assessed over lunch (at 11:45AM), and some questionnaires related to affect and impulsivity (among others) were administered following lunch (between 12:15PM and 3:00PM).

Obtaining Participant Data

Participant records were downloaded from the Collaborative Informatics and Neuroimaging Suite [COINS; (Scott, et al., 2011)] database, in accordance with a Data Use Agreement between The Ohio State University and the Nathan Kline Institute (OSU Agreement No. D16.2131) signed on September 6, 2016. As previously stated, the following inclusion criteria were applied: 1) 18-85 years of age; 2) data release available in BIDS format (resulting in the use of Data Releases 5 through 8 only); 3) available data on height and weight at study enrollment; 4) a completed high-resolution anatomical scan; and 5) a completed diffusion imaging scan that did not exhibit excessive head motion. Of the 1,059 NKI-RS participants with data available through COINS as of September 30, 2016, 275 participants met inclusion criteria for the final sample used in this thesis (n=193 for model building; n=82 for model validation). One participant was excluded due to missing information on height and weight, which is necessary to calculate body mass index (BMI), our primary outcome of interest (n=1,058). Another

142 participants were excluded on the basis of a missing high-resolution anatomical scan (n=916) and 30 additional participants were missing a multiband diffusion imaging scan (n=886), both necessary to assess white matter structural integrity, a primary predictor of interest. We restricted our sample to adults (aged 18-85 years) to reduce the potential for motion artifacts that would interfere with image quality, and to reduce uncertainty with respect to defining cytoarchitectural boundaries in the brain, which are known to undergo considerable change across childhood and adolescence [see (Simmonds, Hallquist, Asato, & Luna, 2014) and (Mills, Goddings, Clasen, Giedd, & Blakemore, 2014)]. Therefore, an additional 313 participants under the age of 18 years and 2 participants without data on current age were excluded prior to analysis (n=571). All 571 remaining subjects had available impulsivity scores, another exposure of interest. Due to time constraints, a subset of participants (those with data in Releases 4-8) were chosen for analysis (Release 4=validation dataset; Releases 5-8=model building dataset). This resulted in the exclusion of an additional 210 participants in Releases 1-3 (n=361). Some T1 and diffusion imaging files were corrupted upon download, rendering 85 affected subjects unusable (n=276). Finally, 1 subject with an implausible BMI value (liberally defined as a BMI<15) was removed from the sample (n=275). Final sample demographics were similar to the larger NKI-RS participant pool with respect to socioeconomic and racial-ethnic characteristics; the most notable difference was the sex distribution (see Table 1).

Physical and Demographic Measures

Height, waist, and hip measurement were recorded to the nearest centimeter by study staff. Weight was recorded in kilograms. Obesity status was classified in binary fashion according to World Health Organization standards (World Health Organization, 2000), such that participants with body mass index (BMI; defined as weight in kilograms divided by squared height in meters) greater than or equal to 30.0 were classified as obese and all other participants were classified as non-obese. Demographics, including age, sex, race, and ethnicity were provided via a self-report questionnaire.

Socioeconomic status (SES) was assessed using the Hollingshead Four Factor Index of Socioeconomic Status (Hollingshead, 1975). This survey measures four facets of SES: marital status, employment status, educational attainment, and occupation type. Retired persons are asked to answer questions related to occupation based on the last time during which they were active in the labor force. Highest education attained is rated on a 7-point scale with the following categories: 1) less than 7^{th} grade; 2) junior high school, including 9^{th} grade; 3) partial high school, up to 11^{th} grade; 4) high school graduate; 5) partial college or at least one year of trade school; 6) standard college/university graduation; and 7) graduate/professional training. Occupational prestige is rated on a 9-point scale with the following categories, defined wherever possible with Census code listings: 1) farm laborers, menial service workers, students, housewives, welfare dependents, and those with no regular occupation; 2) unskilled workers (e.g., food service workers, garbage collectors, gardeners, etc.); 3) machine operators and semi-skilled

workers (e.g., barbers, bus drivers, child care workers, etc.); 4) small business owners (business valued at <$25000), skilled manual laborers (e.g., plumbers, carpenters, electricians, etc.), craftsmen, and tenant farmers; 5) clerical and sales workers or small farm and business owners (business valued at $25000-$50000); 6) technicians, semi-professionals (e.g., court interpreters, clergymen, armed forces, etc.), and small business owners (business values at $50000-$75000); 7) managers, minor professionals, artists and entertainers, and small farm or business owners/operators (business valued at $75000-$100000); 8) administrative officers, commissioned military officers (e.g., lieutenants, captains, etc.), lesser professionals (e.g., nurses, librarians, pilots, etc.), and medium-sized farm owners/operators or business proprietors (business values at $100000-$250000); and 9) higher executives, commissioned military officers (e.g., majors, lieutenant commanders, and above), government officials, major professionals (e.g., engineers, physicians, lawyers, etc.), and large farm owners or business proprietors (business valued at $250000 or more). For participants with spouses/significant others living in the same domicile, partner information about education and occupation were obtained using the same 7-point and 9-point scales, respectively. Additionally, participants were asked similar questions about maternal and paternal [or the primary financial caregiver(s)] educational attainment and occupational status when the participant was aged 16 years. Cumulative status estimation is computed by summing the occupation scale value weighted by a factor of five and the education scale value weighted by a factor of three. For participants with working, live-in partners, status is estimated separately in each person and averaged over both persons. Parental SES is

scored similarly, such that maternal and paternal status is estimated separately and, when two parents were present, averaged.

Typical sleep duration was assessed via actigraphy recordings. These data were collected on waterproof Philips Respironics Actiwatch 2 devices administered to each participant on the morning of their first visit. Participants were instructed to wear these watches on the wrist corresponding to their non-dominant hand continuously until they reported for their second visit. Therefore, the duration of actigraphy data recordings was between 24 hours and 1 week, depending on the time between participant visits. Participants were instructed to press an "event marker" button on the watch immediately prior to going to sleep each evening. An accelerometer records movement continuously throughout the sleep period. These movements were then analyzed via standard actigraphy software, which uses measures of activity counts over time to compute the average minimum total sleep time hours across evening sleep events. The data released by the Nathan Kline Institute do not include information on the average number of days recorded per participant, nor do they include information about the proportion of week days versus weekend days. Previous studies have demonstrated that this is a reliable method of collecting objective sleep quality data (Gironda, Lloyd, Clark, & Walker, 2007). This value was used as an objective measure of typical sleep duration for the present analyses.

Behavioral Measures

The UPPS-P Impulsive Behavior Scale [(Whiteside & Lynham, 2001); (Whiteside, Lynam, Miller, & Reynolds, 2005)] is a self-report questionnaire consisting of 59 items designed to measure five dimensions of impulsivity, which include negative urgency (i.e., the tendency to engage in impulsive behaviors in the face of negative affect and to experience difficulty resisting temptation), premeditation (i.e., engaging in actions before reflecting on their consequences, which may be indicative of inability to delay gratification in the service of larger, distal goals), perseverance (i.e., inability to focus on tasks), sensation seeking (i.e., tending to enjoy and pursue dangerous activities), and positive urgency (i.e., difficulty resisting temptation or impulses in the face of positive affect). Respondents are asked to reflect on their behavior in the past 6 months and to answer scale items, representative examples of which include, "When I feel bad, I will often do things I later regret in order to make myself feel better now" and "I tend to act without thinking when I am really excited". Items are scored on a 4-point Likert scale, ranging from Agree Strongly=1 to Disagree Strongly=4. Items within each of the five subscales are reverse-scored where appropriate (see Appendix A) and summed. The total UPPS-P score is computed by summing each of the five subscale scores. For participants recruited prior to September 15th, 2015, the UPPS-P was completed on site and post-scan between 10:45AM and 12:00PM on Day 2 of data collection. For participants recruited on or after September 15th, 2015, the UPPS-P was completed during an at-home online self-assessment administered after participants' screening visit, but prior to scanning. This may be of interest, given that some participants answered information about

impulsivity prior to being weighed, while other participants responded to the impulsivity questionnaire after being weighed. It is possible that the act of being weighed could have influenced the way in which participants responded to certain items on the UPPS-P [e.g., Item 7: "I have trouble resisting my cravings (for food, cigarettes, etc.)"].

Image Acquisition

All participants were scanned using a study-dedicated Siemens Magnetom TrioTim 3.0 Tesla MRI scanner. During the scan session, participants underwent a high-resolution anatomical scan via a T1-weighted MP-RAGE sequence (TR=1900ms, 1mm isotropic voxels; TA: 4:18) and a multiband echo planar diffusion sequence in which images were collected via 64 contiguous 2mm thick transverse slices with 137 diffusion directions (TE=85ms, TR=2400ms, b-value=1500s/mm^2, 212mm FOV, 90° flip angle, 2mm isotropic voxels, multiband accelerator factor: 4; TA: 5:58), as well as other imaging protocols not directly relevant to the present hypotheses. Multiband imaging allows for expedited sampling rates while still achieving full-brain coverage, because multiple image slices are obtained simultaneously, thereby significantly reducing the total time needed to complete the sequence (Feinberg & Setsompop, 2013).

Defining Seed, Waypoint, and Exclusion Masks

Left and right nucleus accumbens (NAcc) masks were derived via FSL's FIRST, a fully-automated subcortical structural segmentation and registration tool (Patenaude, Smith, Kennedy, & Jenkinson, 2011). FIRST yields the most likely shape for each subcortical structure based on multivariate Gaussian assumptions and training data correspondence, in light of a given subject's observed T1-weighted image intensities. In simplified terms, the program uses anatomical landmarks in the brain to make a "best guess" for the boundaries of a given neural structure, based on independent leave-one-out cross validation data used to develop the segmentation algorithm. Subcortical parcellations were visually inspected, and no glaring distortions or misclassifications in delineation were detected. Each NAcc segmentation was saved as a binarized mask, which was then used as a seed region during the extraction of tract-based spatial statistics.

A bilateral orbitofrontal cortex (OFC) mask was obtained from Neurosynth, a platform that automatically yields a pictorial meta-analysis of neural architecture based on previous peer-reviewed publications on functional neuroimaging data (Yarkoni, Poldrack, Nichols, Van Essen, & Wager, 2011). The extracted cortical mask was derived using a reverse inference map, which corresponds to the likelihood that the term "orbitofrontal" (n=682 studies) was used in a study given a voxel exhibits activation change. The resulting orbitofrontal cortical map was thresholded to correct for multiple comparisons using a 0.01 criterion for voxelwise false discovery rate. An additional

criterion was imposed, such that any given voxel must have been reported in at least five previous studies to meet inclusion criteria for mask generation. Images were then downloaded and binarized. Next, this preliminary orbitofrontal mask was edited such that all voxels posterior (in MNI space, $y<80$) or dorsal (in MNI space, $z>35$) to the anterior cingulate genu were excluded. Finally, to ensure that probabilistic tractography analyses captured only ipsilateral connections between each nucleus accumbens and the orbitofrontal cortex, we generated an exclusion mask at the midline (3 slices thick, centered at $x=45$ in MNI space). The edited orbitofrontal mask and exclusion mask were then warped into subject-specific T1 structural space for all subjects assigned to the training dataset (n=193). These warped images were then used as waypoint (OFC) and exclusion regions, respectively, during probabilistic tractography analyses.

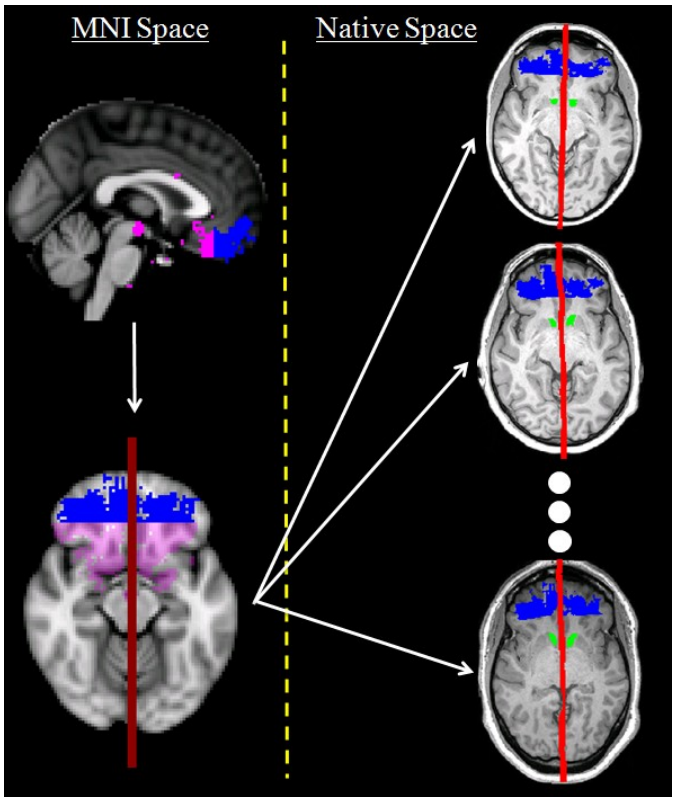

Figure 1. Warping Masks from Standard to Native Space
A pictorial representation of seed, waypoint, and exclusion mask creation. An orbitofrontal (OFC) mask was downloaded from Neurosynth based on reverse inference from a meta-analysis of 682 studies using the term "orbitofrontal", where a given voxel represents a minimum of five studies. Purple colors indicate the originally downloaded mask. Dark blue colors in the left column, which indicates stereotaxic space, represent the truncated OFC mask created for this thesis. All voxels posterior to y=80 or dorsal to z=35 in MNI space were deleted (as indicated by the translucent purple). An exclusion mask 3 slices thick was created at the midline, centered at x=45 in MNI space (indicated in dark red). Voxels indicated in dark blue and dark red were then warped into each subject's native space (right panel). FSL's FIRST was used to automatically parcellate each subject's bilateral nucleus accumbens (indicated in green).

Preprocessing and Probabilistic Tractography

Diffusion-weighted images from 275 participants were preprocessed using standard procedures implemented in FSL's Diffusion Toolbox [FDT; (Behrens, et al., 2003)], including brain extraction via skull-stripping and eddy current and head motion corrections. Distortions due to head motion were corrected using affine registration

(Jenkinson, Bannister, Brady, & Smith, 2002) by aligning diffusion-weighted images to the average of the nine non-diffusion-weighted images (i.e., b0 images). We took extra precaution to prevent spurious results from unreliable diffusivity measurement driven by excessive head motion; we evaluated the extent of motion distortion within 6 parameters [3 translation (i.e., along x- y- and z-axes) and 3 rotation (i.e., pitch, roll, and yaw)] by calculating their combined root mean square (RMS) deviation volume-by-volume, derived from the pairwise divergence between the affine registration of each volume to the mean of each of the nine b0 images. The average of all pairwise deviations yields a summary statistic for head motion for each participant. Any participant with an average RMS exceeding 1.5mm was excluded from subsequent analyses.

We used probabilistic tractography to delineate white matter pathways between the bilateral NAcc and the OFC, excluding fibers crossing through the midline. First, nucleus accumbens seed masks, orbitofrontal waypoint masks, and midline exclusion masks were warped into each subject's native diffusion space. Then, tractography maps were generated via single-mask seeding using 5,000 probabilistic streamlines per voxel using FSL's BEDPOSTx (Behrens, Berg, Jbabdi, Rushworth, & Woolrich, 2007) ,which accounts for uncertainty in the diffusion imaging signal created by crossing fibers. In so doing, only streamlines that pass through *both* subcortical and cortical seed regions in a given subject were retained. Each subject-specific probabilistic pathway within the training dataset was binarized and then warped into standard MNI stereotaxic space using FNIRT, a non-linear registration process. All model-building participants' probabilistic tracts were then aggregated into two group-level masks (one corresponding to each left

and right hemisphere), such that consistency was ensured by specifying that at least 95% of all participants had probabilistically-defined white matter pathways at any given voxel included in the group masks. This group-defined pathway was then warped back into each subject's native diffusion space and superimposed on each subject's fractional anisotropy (FA) structural image. From here, FA within the group-defined pathways was thresholded at ≥0.20 to ensure that extracted values truly represent white matter morphometry. Following thresholding, mean FA within each tract was obtained, and this value corresponds to each subject's structural integrity "exposure level".

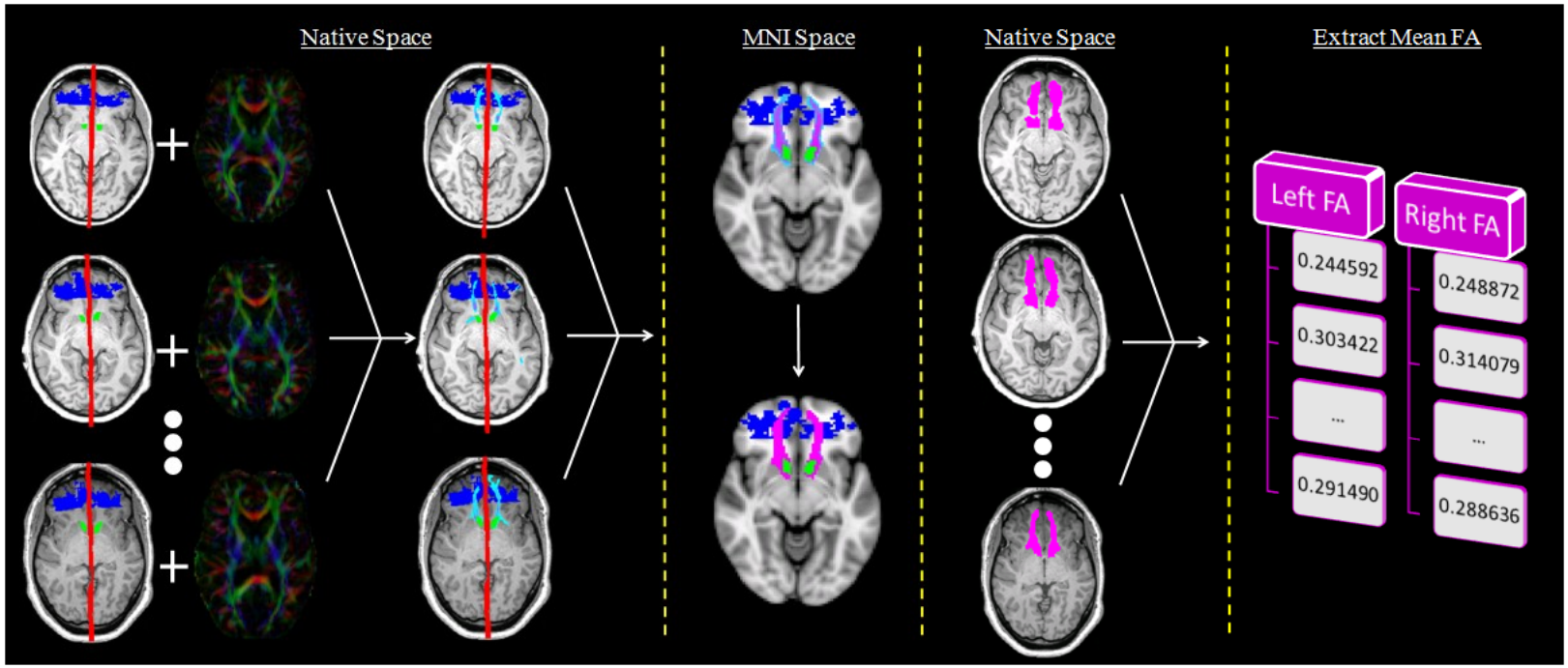

Figure 2. Process for Extracting Mean Fractional Anisotropy

A pictorial representation of tractography, creation of a probabilistic group-threshholded mask of each tract, and extraction of mean fractional anisotropy (FA) within tracts. Seed (green), waypoint (dark blue), and exclusion (dark red) masks in each subject were non-linearly transformed (addition signed) to preprocessed fractional anisotropy maps (second column in native space; FA maps color-coded to represent fiber orientations) prior to probabilistic tractography analyses. 5,000 probabilistic streamlines per nucleus accumbens (green) voxel passing through the orbitofrontal cortex (dark blue), but not passing through the exclusion mask (dark red) were used to estimate a white matter pathway for each subject in each hemisphere (cool colors in last column of first "native space" division). These pathways were then warped into standard space (top image of MNI column) and binarized (bottom image of MNI column; solid purple). All of these binarized tracts were summed and a group-threshholded tract representing probabilistically-defined pathways in 95% of participants or more was created. This group tract was then warped back into each subject's native diffusion space (division 3; solid purple). Mean FA in each of these tracts was extracted after excluding voxels with FA<0.20 (presumed not to represent white matter; final division).

Finally, based on prior work (Chen, Chavez, & Heatherton, 2016), we had an a priori hypothesis that a white matter pathway connecting the left orbitofrontal cortex (lOFC) to the left inferior frontal gyrus (lIFG) might function as an inhibitory connection, related to individuals' ability to resist impulses arising from appetitive cues. We contacted Chen and colleagues, who generously provided their group-thresholded left OFC-IFG tract mask (defined via a food-cue reactivity task conducted in 36 female dieters undergoing functional magnetic resonance imaging) in MNI space. Upon discovering that the OFC-IFG tract and OFC-NAcc tract were partially overlapping, we eliminated any voxels represented in both tracts from the analyses.

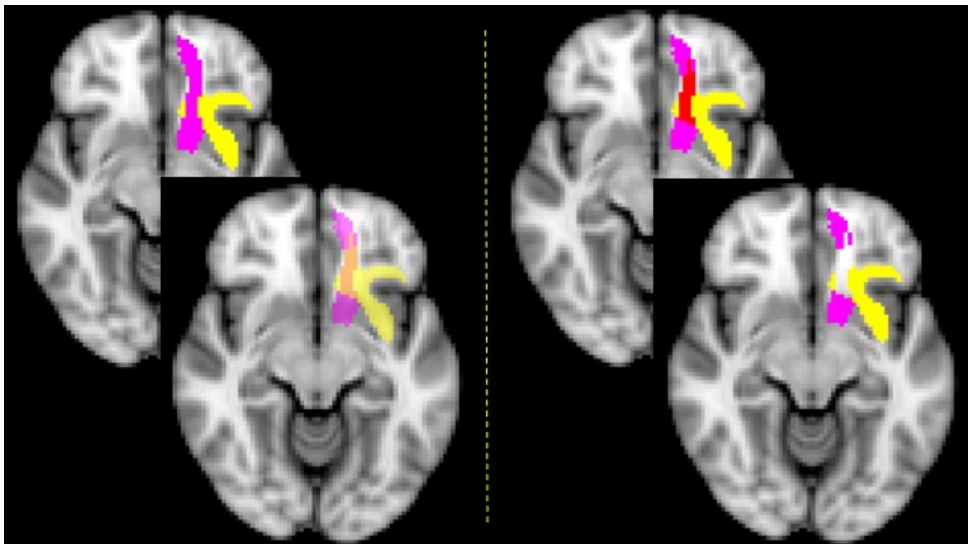

Figure 3. Addressing the Issue of Overlapping White Matter Tracts
A pictorial representation (at z=31 in MNI space) of the overlap between the left nucleus accumbens (NAcc) to left orbitofrontal (OFC) tract (purple) and the left OFC to left inferior frontal gyrus (IFG) tract (yellow). The bottom image to the left of the division line indicates the extent of the overlap by making each tract translucent. Voxels represented in both tracts (indicated in red, to the right of the division line) were removed prior to extracting mean fractional anisotropy (FA) values in either left-lateralized tract. The bottom image to the right of the division line indicates the final left NAcc to left OFC tract (purple) and the final left OFC to left IFG tract (yellow).

Following elimination of overlapping voxels, a procedure identical to the one described above was used to warp this OFC-IFG group-defined mask into native space for each subject included in the present analyses, and from there, to extract his/her mean FA within the pathway.

Analytic Strategy

A logistic regression model was built on the training dataset, which included participants in Data Releases 5 through 8 (n=193), using a predictive modeling approach. First, univariable logistic regression analyses were performed to predict the log-odds of obesity as a function of age, sex, racial-ethnic background, parental socioeconomic status, average sleep duration, impulsivity, and integrity of each white matter pathway, respectively. A decision criterion of 0.20 was set for each likelihood ratio chi-square p-value, such that variables with this significance level or below were retained in subsequent analyses. However, due to our particular interest in assessing the effect of white matter integrity on the odds of obesity, we decided prior to model building that mean FA for at least one pathway connecting each region (regardless of hemisphere lateralization) would be retained in the final model. Additionally, due to known changes in global FA with age, we predetermined that this covariate would remain in the final multivariable model. Any variable meeting our a priori cutoff of p=0.20 was entered into a multivariable logistic regression model. Backward selection was used to remove variables in an iterative fashion. Fractional polynomials were used on all continuous

measures to determine whether their relationship to obesity was linear in the logit; non-linear terms were added where appropriate, with an effort to balance warranted model complexity with parsimony and ease of interpretability. All possible interactions with the remaining variables were generated and allowed the opportunity to enter the model using forward selection with an inclusion criteria of p=0.05.

Model fit was assessed using both Pearson chi-square and Hosmer-Lemeshow tests for goodness of fit. Sensitivity and specificity of the model were graphed across all potential probability cut points and the classification accuracy for models using a variety of cut points around the intersection of sensitivity and specificity were explored. The cut point corresponding to the probability of obesity that best maximized sensitivity and specificity in the training dataset was chosen to test the efficacy of the model's ability to predict the obesity status of participants in the holdout sample (n=82).

Model discrimination was assessed by deriving the area under the receiver operating characteristic curve (AUC) and using nonparametric bootstrapped receiver operating characteristic regression estimation with 500 replicates to construct a confidence interval around the AUC. The bounds of this interval were used to determine the discriminability of the model qualitatively using generally accepted rules of thumb (Hosmer & Lemeshow, 2000).

Model diagnostics were performed by examining covariate patterns that had high leverage, large standardized residuals, and/or high influence [a standardized measure of influence analogous to Cook's distance called Pregibon's $\Delta\hat{\beta}$; (Pregibon, 1981)] was used

to assess the effect that a given covariate pattern exerted on the estimated regression coefficients produced by the final model. Covariate patterns identified as outliers, which we define as exhibiting extreme values on any of these three diagnostic metrics, were first checked for biological plausibility and coding errors. Next, these outlying covariate patterns were removed from the model iteratively. After removing each extreme covariate pattern, the model was refit with the remaining training data and changes in coefficient estimates were examined. Any change-in-estimate exceeding 20% was flagged.

The final model was tested on a holdout sample (n=82), and the predicted probability of obesity (i.e., the fitted values) was generated for each participant in this validation dataset. Model validation was performed by applying the cut point that best maximized sensitivity and specificity in the training dataset to the holdout sample. The cut point was used as a binary decision criterion whereby each subject was classified as either obese (at or above the cut point) or non-obese (below the cut point). These classifications were then compared to each participant's true obesity status. Sensitivity, specificity, and classification accuracy within the holdout sample were computed based on the correspondence, or lack thereof, of the predicted and true obesity status for each holdout sample participant.

Finally, the model was refit in the training dataset twice, following the same steps described above, to illustrate the deleterious effects of failing to take an interdisciplinary approach. In one instance, neural predictors were excluded as possible explanatory

variables. In the other instance, sociodemographic predictors were excluded as possible explanatory variables. Sensitivity, specificity, and classification accuracy of the full model was compared to each of these refitted models, to demonstrate to epidemiologists and neuroscientists alike the added benefits of considering sources of variability at both biological and sociological levels.

Results

The distribution of BMI in the model building dataset (see figure below) is roughly representative of the distribution of BMI in the United States (Flegal, Carroll, Kit, & Ogden, 2012); it peaks just before a BMI of 25 and exhibits the characteristic right skew we would expect. The distribution of each potential explanatory variable was explored in relationship to obesity prevalence and impulsivity (see **Table 2**).

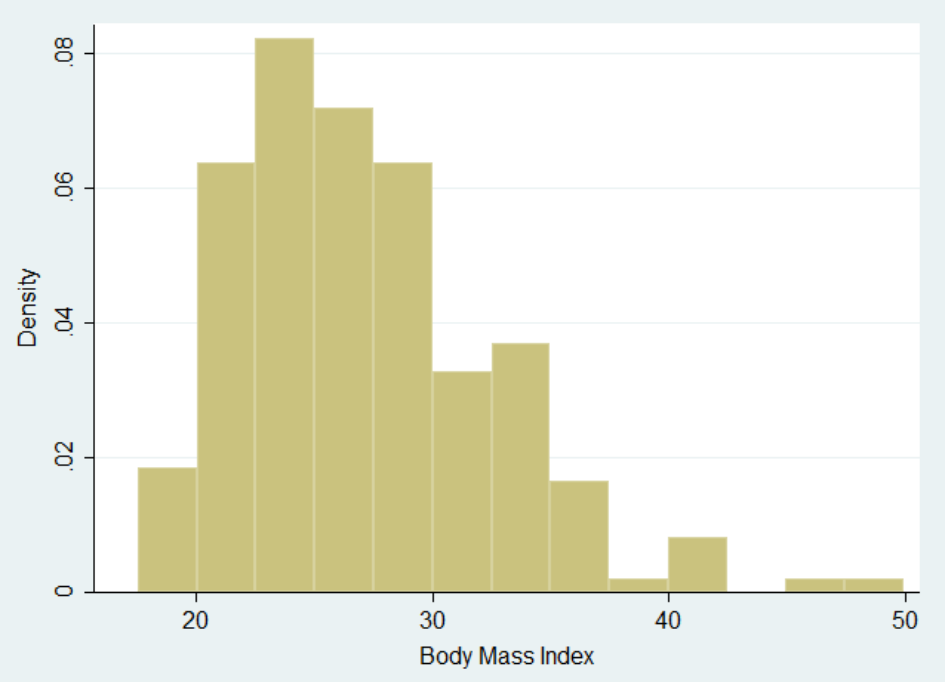

Figure 4. Distribution of BMI in the Model Building Dataset
Histogram of body mass index (BMI) in the model building dataset for this thesis, which represents 195 subjects in the Enhanced Nathan Kline-Rockland Sample in Releases 5 through 8. Bar height represents the proportion of the sample falling into a given BMI bin, represented by bar width.

	Total Sample N (%)	Obese (BMI≥30) N (%)	Impulsivity Mean (Std)
Overall	195 (100.00%)	49 (25.13%)	109.97 (1.43)
Combined Race/Ethnicity			
Non-Hispanic Asian	8 (4.10%)	1 (12.50%)	120.00 (12.51)
Non-Hispanic Black or African American	31 (15.90%)	9 (29.03%)	110.23 (20.84)
Non-Hispanic White	131 (67.18%)	32 (24.43%)	107.59 (19.06)
Non-Hispanic Other Race	3 (1.54%)	1 (33.33%)	121.33 (25.72)
Hispanic, Any Race	22 (11.28%)	6 (27.27%)	118.59 (23.55)
Sex			
Male	51 (26.15%)	18 (35.29%)	116.73 (18.99)
Female	144 (73.85%)	31 (21.53%)	107.58 (19.91)
Age			
18-24 Years	39 (20.00%)	7 (17.95%)	121.23 (19.66)
25-44 Years	64 (32.82%)	22 (34.38%)	113.16 (19.75)
45-64 Years	53 (27.18%)	11 (20.75%)	101.42 (18.99)
65-85 Years	39 (20.00%)	9 (23.08%)	105.10 (15.80)
Parents' SES			
1st Quartile SES	47 (25.00%)	14 (29.79%)	107.06 (3.13)
2nd Quartile SES	46 (24.47%)	14 (29.17%)	109.81 (2.60)
3rd Quartile SES	46 (24.47%)	11 (22.45%)	112.33 (2.95)
4th Quartile SES	49 (26.06%)	7 (15.91%)	111.93 (3.04)
Average Sleep Duration			
<5 Hours	26 (16.25%)	11 (42.31%)	114.88 (21.30)
5-7 Hours	90 (56.25%)	25 (27.78%)	107.50 (19.10)
>7 Hours	44 (27.50%)	7 (15.91%)	109.55 (23.47)
Left "Reward Tract"			
1st Quartile Mean FA	49 (25.39%)	12 (24.49%)	104.39 (2.80)
2nd Quartile Mean FA	48 (24.87%)	11 (22.92%)	109.46 (2.90)
3rd Quartile Mean FA	48 (24.87%)	12 (25.00%)	112.40 (3.27)
4th Quartile Mean FA	48 (24.87%)	13 (27.08%)	113.56 (2.48)
Left "Inhibitory Tract"			
1st Quartile Mean FA	49 (25.39%)	16 (32.65%)	105.24 (2.75)
2nd Quartile Mean FA	48 (24.87%)	15 (31.25%)	107.46 (2.82)
3rd Quartile Mean FA	48 (24.87%)	9 (18.75%)	113.50 (3.05)
4th Quartile Mean FA	48 (24.87%)	8 (16.67%)	113.58 (2.85)

Table 2. Descriptive Statistics (Overall and by Obesity Status and Impulsivity)

Features of the distributions of obesity and impulsivity (UPPS-P Impulsive Behavior Scale total score) as a function of other potential covariates. Parents' socioeconomic status is measured via the Hollingshead Four-Factor Index of Socioeconomic Status. Average sleep duration is measured via averaged actigraphy recordings over the course of 24hrs to 1wk. Variable sample size per row (195-160; due to missing data).

As illustrated in Table 2, we see an unexpected association between sex and obesity, such that men are more likely to be obese than women. This may be due, in part, to the skewed sex distribution in the portion of the Rockland Sample used for this thesis (i.e., see Table 1; 73.1% of participants are female). As expected, we can see that obesity seems to peak in middle age (Flegal, Carroll, Kit, & Ogden, 2012), and lower socioeconomic status is associated with higher rates of obesity (Sobal & Stunkard, 1989). The expected association between shorter sleep duration and increased obesity prevalence (Cappuccio, et al., 2008) is also observed in the model building dataset. As anticipated, men seem more likely to report higher levels of impulsivity than women (Cross, Copping, & Cambell, 2011). Similarly, the predicted association between age and impulsivity (Steinberg, Albert, Cauffman, Banich, Graham, & Woolard, 2008), whereby younger participants are more likely to report higher levels of impulsivity than older participants, is observed. Additionally, integrity of the white matter pathway connecting the left orbitofrontal cortex to the left inferior frontal gyrus (the "inhibitory pathway") seems to be inversely associated with the prevalence of obesity (i.e., greater integrity of the inhibitory pathway is protective against obesity). Also of note, integrity of the white matter pathway connecting the left nucleus accumbens to the left orbitofrontal cortext (the "reward pathway") seems to be positively associated with self-reported impulsivity (i.e., a stronger reward pathway is linked to greater impulsive behavior).

Model Building

The table below displays the results of our first-pass univariable analyses for predicting the log odds of obesity (BMI ≥ 30), such that inclusion decisions are denoted with a check mark and exclusion decisions are denoted with an empty circle.

Variable	$\hat{\beta}$	$\widehat{SE}(\hat{\beta})$	$\widehat{OR}$	95% CI	Log-Likelihood	p-value	Decision
Age (in years)	-0.0057	0.0089	0.9943	(0.98, 1.01)	-109.72	0.5196	✓
Racial-Ethnic Group					-109.32	0.8753	O
Non-Hispanic Asian	-0.8165	1.0882	0.4420	(0.05, 3.73)			
Non-Hispanic Black	0.2356	0.4449	1.2656	(0.53, 3.03)			
Non-Hispanic Other Race	0.4362	1.2415	1.5469	(0.14, 17.63)			
Hispanic, Any Race	0.1486	0.5201	1.1602	(0.42, 3.22)			
Sex	0.6873	0.3563	1.9883	(0.99, 4.00)	-108.12	0.0569	✓
Average Hours Sleep/Night - Actigraphy	-0.2673	0.1253	0.7655	(0.60, 0.98)	-90.68	0.0271	✓
UPPS-P Total Impulsivity Score	0.0220	0.0084	1.0223	(1.01, 1.04)	-106.40	0.0079	✓
Parents' SES at 16yrs	-0.0228	0.0137	0.9774	(0.95, 1.00)	-103.22	0.0954	✓
Mean FA – Tract 1 (rOFC ←→ rNAcc)	-0.8885	5.5879	0.4113	(0.00, 23473.37)	-108.24	0.8737	✓
Mean FA – Tract 2 (lOFC ←→ lNAcc)	-1.1993	6.4109	0.3014	(0.00, 86332.43)	-108.24	0.8516	✓
Mean FA - Tract 3 (lOFC ←→ lIFG)	-13.1799	5.0498	0.0000	(0.00, 0.04)	-104.72	0.0078	✓

Table 3. Univariable Analyses

Univariable logistic regression analyses for predicting the log-odds of obesity in the model building dataset (n=195). Any variables with p-values at or below 0.20 were retained, as well as all predictors corresponding to white matter pathways (of particular interest in this study) and age (known to be related non-linearly to other covariates of interest).

The full model therefore took the following form:

$$\boldsymbol{Full\ Model}: \widehat{\boldsymbol{g}}(\boldsymbol{x}) = \widehat{\boldsymbol{\beta_0}} + \widehat{\boldsymbol{\beta_1}}(\boldsymbol{age}) + \widehat{\boldsymbol{\beta_2}}(\boldsymbol{sex}) + \widehat{\boldsymbol{\beta_3}}(\boldsymbol{sleep}) + \widehat{\boldsymbol{\beta_4}}(\boldsymbol{impulsivity}) + \widehat{\boldsymbol{\beta_5}}(\boldsymbol{parses}) + \widehat{\boldsymbol{\beta_6}}(\boldsymbol{FA\ tract\ 1}) + \widehat{\boldsymbol{\beta_7}}(\boldsymbol{FA\ tract\ 2}) + \widehat{\boldsymbol{\beta_8}}(\boldsymbol{FA\ tract\ 3})$$

Using multivariate Wald statistics, variables were deleted, one by one, that did not meaningfully contribute to predicting the log-odds of being obese. After deleting each variable, we fit a reduced model without the eliminated variable and compared it to the last iteration of our full model to assess the significance, using a likelihood ratio test, of the variable removed. First, we removed the variable corresponding to mean fractional anisotropy of the white matter pathway connecting the right nucleus accumbens to the right orbitofrontal cortex. A likelihood ratio test indicated that this reduced model did not perform significantly worse than the full model: $LR\ \chi^2(1) = 0.92, p = 0.34$. Next, we removed the variable corresponding to actigraphy-measured average hours of sleep per night. Again, a likelihood ratio test indicated that this reduced model did not perform significantly worse than the full model: $LR\ \chi^2(1) = 1.57, p = 0.21$. Following this iteration, all variables (except age, which was retained based on prior knowledge) were significant at or below our a priori cutoff level of 0.1, so they were retained for further analysis. Therefore, the reduced model took the following form:

$$\boldsymbol{Reduced\ Model}: \widehat{\boldsymbol{g}}(\boldsymbol{x}) = \widehat{\boldsymbol{\beta_0}} + \widehat{\boldsymbol{\beta_1}}(\boldsymbol{age}) + \widehat{\boldsymbol{\beta_2}}(\boldsymbol{sex}) + \widehat{\boldsymbol{\beta_3}}(\boldsymbol{impulsivity}) + \widehat{\boldsymbol{\beta_4}}(\boldsymbol{parses}) + \widehat{\boldsymbol{\beta_5}}(\boldsymbol{FA\ tract\ 2}) + \widehat{\boldsymbol{\beta_6}}(\boldsymbol{FA\ tract\ 3})$$

As a precautionary measure, we added back into the model the only variable not originally selected from the univariable analyses presented earlier (i.e., racial-ethnic background). This variable did not add any significant predictive information about the log-odds of obesity, so the reduced model above was retained: $LR\ \chi^2(3) = 1.65, p = 0.65$.

Fractional polynomials indicated that, for most continuous variables (i.e., impulsivity, parents' SES, FA in tract 2, and FA in tract 3), the best higher-order terms did not significantly improve model fit relative to the more parsimonious linear parameterization. However, with respect to the predictor corresponding to participant age, the best m=2 model was somewhat better than the best m=1 model (best m=2 model corresponds to powers of -2 and -2; p=0.269). After comparing the best m=2 model with an easier-to-interpret m=2 model (i.e., corresponding to powers 1 and -1) that seemed to perform similarly (based on comparable model deviance), we constructed a non-linear term for age corresponding to the inverse of age, and entered it into the reduced model above. The addition of a term for the inverse of age provided marginally significant predictive information above and beyond the linear main effects model: $LR\ \chi^2(1) = 3.19, p = 0.07$. Therefore, the final main effects model took the following form:

$$\boldsymbol{Main\ Effects\ Model}: \widehat{\boldsymbol{g}}(\boldsymbol{x}) = \widehat{\boldsymbol{\beta_0}} + \widehat{\boldsymbol{\beta_1}}(\boldsymbol{age}) + \widehat{\boldsymbol{\beta_2}}\left(\frac{\boldsymbol{1}}{\boldsymbol{age}}\right) + \widehat{\boldsymbol{\beta_3}}(\boldsymbol{sex}) + \widehat{\boldsymbol{\beta_4}}(\boldsymbol{impulsivity}) + \widehat{\boldsymbol{\beta_5}}(\boldsymbol{parses}) + \widehat{\boldsymbol{\beta_6}}(\boldsymbol{FA\ tract\ 2}) + \widehat{\boldsymbol{\beta_7}}(\boldsymbol{FA\ tract\ 3})$$

No interaction terms fell below our a priori significance level of 0.05. Therefore, the main effects model above was retained as the final model, which has been reproduced below with its corresponding coefficient estimates. Additionally, a table describing this final model is provided below.

$$\boldsymbol{Final\ Model}: \widehat{\boldsymbol{g}}(\boldsymbol{x}) = \boldsymbol{5.83 - 0.06(age) - 80.61}\left(\frac{\boldsymbol{1}}{\boldsymbol{age}}\right) \boldsymbol{+ 0.99(sex) + 0.03(impulsivity) - 0.04(parses) + 43.14(FA\ tract\ 2) - 48.76(FA\ tract\ 3)}$$

Variable	$\hat{\beta}$	$\widehat{SE}(\hat{\beta})$	$\widehat{OR}$	95% CI	Wald p-value
Constant	5.8260	4.3061			
Age (in years)	-0.0566	0.0314			0.071
Inverse Age (in years)	-80.6123	46.5174			0.083
Sex (Female=Referent)	0.9860	0.4603	2.6806	(1.09, 6.61)	0.032
UPPS-P Total Impulsivity Score*	0.0324	0.0112	1.3820	(1.11, 1.72)	0.004
Parents' SES at 16 Years*	-0.0375	0.0159	0.6872	(0.50, 0.94)	0.018
Mean FA – Tract 2 (lOFC ←→ lNAcc)#	43.1353	14.2769	1.5393	(1.16, 2.04)	0.003
Mean FA - Tract 3 (lOFC ←→ lIFG)#	-48.7592	11.0925	0.6141	(0.49, 0.76)	<0.0005

Table 4. Final Model Parameters

Parameterization of the final predictive model for the log-odds of obesity, including coefficient estimates and their associated standard errors, 95% confidence intervals, and significance levels.

* Odds ratios and 95% CIs correspond to a 10-unit increase in impulsivity or indexed SES

Odds ratios and 95% CIs correspond to a 0.01-unit increase in mean fractional anisotropy

Interpretation of Model Coefficients

Based on the training set data, we observe a strong positive association between impulsivity and the odds of obesity, such that a 10-unit increase on the UPPS-P Impulsive Behavior Scale was associated with a 38% increase in the odds of obesity, holding constant age, sex, parental SES, and mean FA in each white matter pathway. Mean FA in the tract connecting the left OFC to the left NAcc, which we operationalize as a "reward pathway", is also positively associated with the odds of obesity, such that a 0.01-unit increase in mean FA in this tract predicts a 54% increase in the odds of obesity, controlling for all other variables in the model. Conversely, mean FA in the tract connecting the left OFC to the left IFG, which we operationalize as an "inhibitory pathway", is inversely associated with the odds of obesity; for each 0.01-unit increase in mean FA within this pathway, we observe a 39% decrease in the odds of obesity, controlling for all other variables in the model. It is noteworthy that mean FA in the two

white matter pathways are highly correlated (r=0.76; see Table 5 below for complete correlation matrix; see Figure 5 for correlation between white matter tracts). Therefore, the interpretation of a coefficient associated with a white matter pathway should be in the context of the other pathway (e.g., Given two individuals have the same "reward pathway" mean FA, what is the effect of a 0.01-unit difference in mean FA of the "inhibitory pathway"?).

	Age	Sex	Impulsivity	Parents' SES	OFC←→NAcc	OFC←→IFG
Age	1.00					
Sex	-0.14	1.00				
Impulsivity	-0.35	0.22	1.00			
Parents' SES	-0.15	0.10	0.08	1.00		
OFC←→NAcc	-0.50	-0.03	0.14	0.06	1.00	
OFC←→IFG	-0.49	0.09	0.17	0.06	0.76	1.00

Table 5. Correlation Matrix for Final Model Covariates

Matrix of correlations for each covariate included in the final model predicting the log-odds of obesity. Matrix corresponds to a sample size of 186 participants (i.e., only those participants with available data on every covariate).

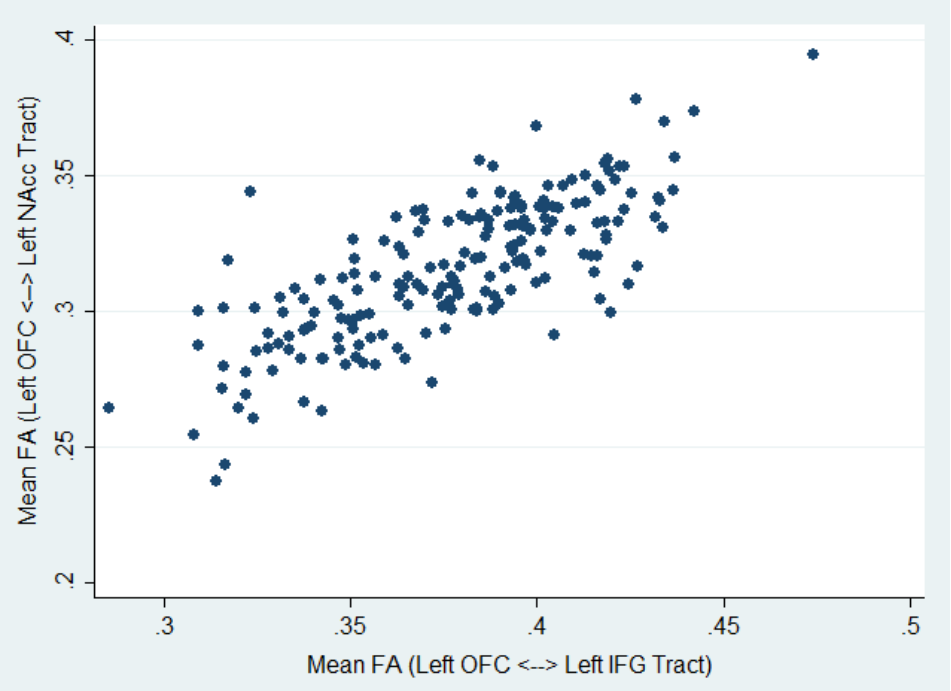

Figure 5. Correlation Between Integrity of "Inhibitory" and "Reward" Pathways
Scatterplot of mean fractional anisotropy (FA) in the white matter pathway connecting the left orbitofrontal cortex (OFC) to the left inferior frontal gyrus (IFG) on the x-axis and mean FA in the white matter pathway connecting the left OFC to the left nucleus accumbens (NAcc) on the y-axis. Though mean FA in these two tracts are highly correlated (r=0.76), there is still considerable variability to be explained.

With respect to socioeconomic and demographic predictors, the model suggests the following interpretations. A male's odds of obesity are 2.68 times that of a female. This odd finding may be related to the skewed sex distribution in the portion of the Rockland Sample used for this thesis (see column 5 of **Table 1**). For every 1-unit increase in parents' educational and occupational status when the participant was 16 years of age, we expect a corresponding decrease of 3.7% in the odds of obesity. And finally, the relationship between age and the probability that an individual is obese seems to be nonlinear. To illustrate, consider a hypothetical male with average impulsivity (≈110), average parental (≈43), average mean FA in the "reward pathway" (≈0.32), and

average mean FA in the "inhibitory pathway" (≈0.38). The plot below describes the probability of obesity for this hypothetical male at a range of possible ages represented in the sample data.

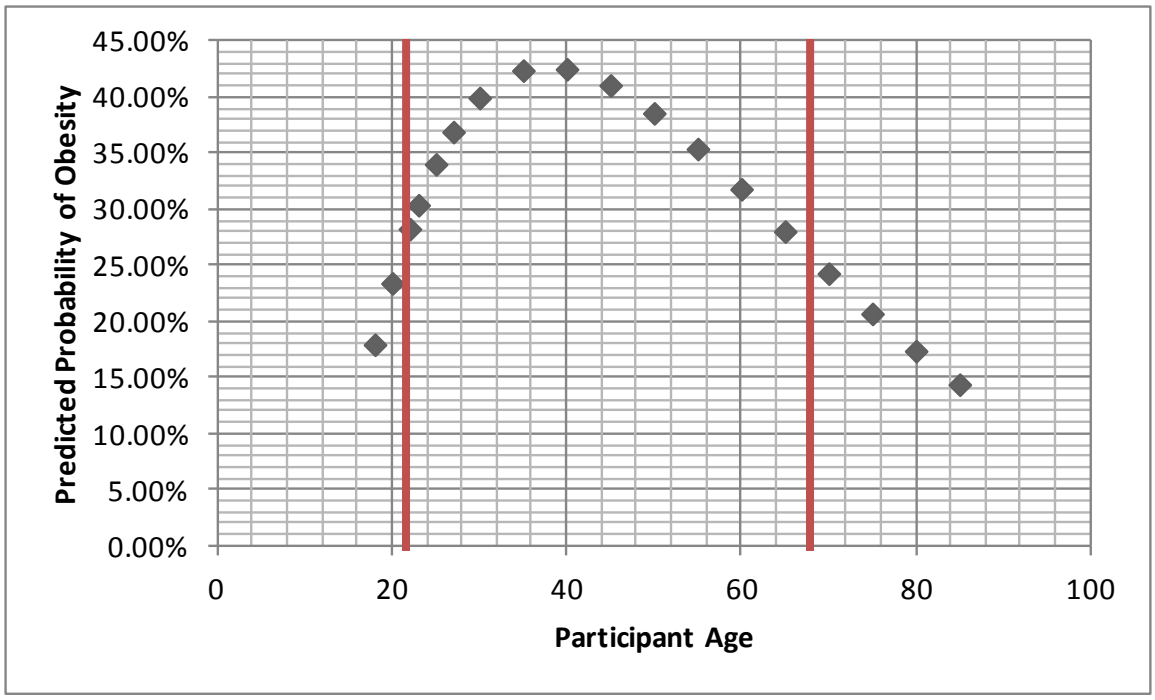

Figure 6. Predicted Probability of Obesity as a Function of Age for Hypothetical Male Subjects with All Other Covariates Held Constant

Illustration of the non-linear association between age and the probability of obesity. Figure represents the probability of obesity for hypothetical male subjects with average self-reported impulsivity, average parental socioeconomic status (SES), average mean FA in the pathway connecting the left nucleus accumbens to the left orbitofrontal cortex (OFC), and average mean FA in the pathway connecting the left OFC to the left inferior frontal gyrus. Participants with different covariate values (e.g., females, those with high parental SES, etc.) will have identical probability curves shifted either up or down. Portions of the function within the red bars correspond to values of age at which the model would classify a male with these covariate values as obese; portions of the function outside of the red bars correspond to values of age at which the model would classify a male with these same covariate values as non-obese.

Model Fit, Adequacy and Discrimination

Both a Pearson chi-square test and a Hosmer-Lemeshow test for goodness-of-fit converge in their indication that our final model fits the data well: Pearson $\chi^2(178) = 200.34, p = 0.12$; Hosmer-Lemeshow $\chi^2(8) = 8.35, p = 0.40$. The figure and table below detail the sensitivity and specificity estimates for classifying participants as being obese or non-obese using a variety of cut-off values for the probability of being obese.

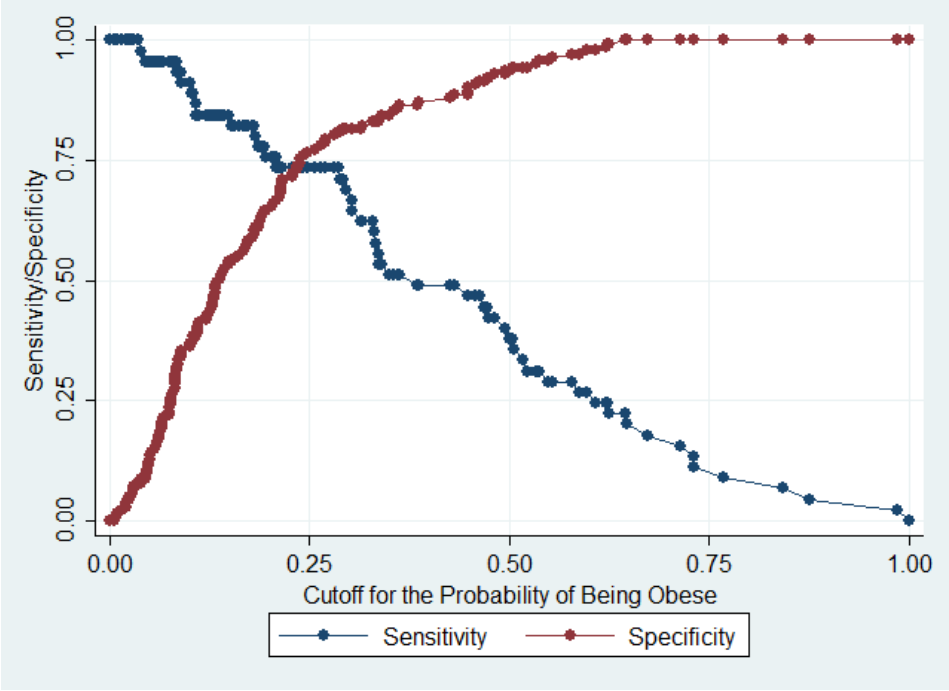

Figure 7. Final Model: Graph of Sensitivity and Specificity vs. Probability Cutoffs
Illustration of the intersection of sensitivity (predicting a given person is obese when s/he is obese) and specificity (predicting a given person is not obese when s/he is not obese). The point at which both sensitivity and specificity are maximized was chosen as the cutoff for the probability of being obese used in the holdout sample.

Cut-off	*Sensitivity*	*Specificity*	*Correctly Classified*
0.15	82.22%	53.90%	60.75%
0.20	75.56%	65.25%	67.74%
0.22	73.33%	71.63%	72.04%
0.24	73.33%	75.89%	75.27%
0.26	73.33%	78.01%	76.88%
0.27	**73.33%**	**80.14%**	**78.49%**
0.28	73.33%	80.14%	78.49%
0.30	66.67%%	81.56%	77.96%
0.35	51.11%	84.40%	76.34%

Table 6. Sensitivity, Specificity, and Classification Accuracy as a Function of Probability Cutoffs

Performance of the final model in the training dataset for sensitivity, specificity, and overall classification accuracy at a variety of potential decision cut points for predicting the probability of being obese.

With respect to our later goal of model validation, the figure and table above indicate that the optimal classification cutoff for the probability of being obese that maximizes both sensitivity and specificity is around 0.27. Using the model-building dataset as a guide, we can expect that this cutoff would result in the correct classification of approximately 78.49% of participants.

The area under the receiver operating characteristic (ROC) curve, reproduced below, was used to assess the discriminability of the model.

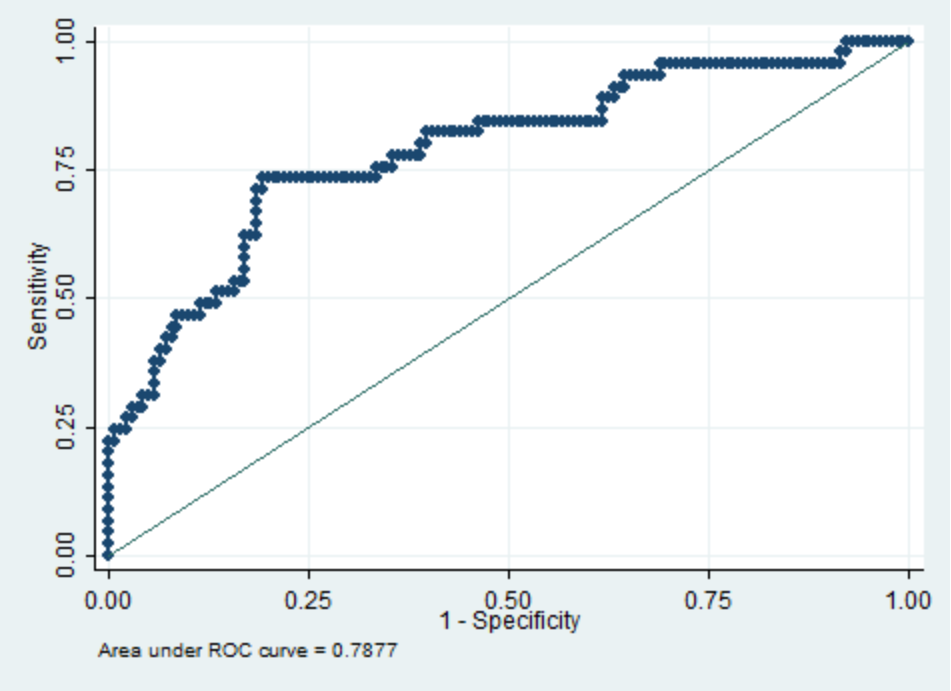

Figure 8. Final Model: Receiver Operating Characteristic Curve
Illustration of the area under the receiver operating characteristic curve for the performance of the final model in the training dataset.

Given that the area under the ROC curve is equal to 0.7877 (95%CI: 0.6798, 0.8365), we can conclude that this model has acceptable to excellent discrimination (Hosmer & Lemeshow, 2000).

Model Diagnostics

All leverage values were relatively low ($h<0.15$ for all covariate patterns; see figure below). For the sake of completeness, the covariate patterns associated with the highest three leverage estimates were flagged for later inspection.

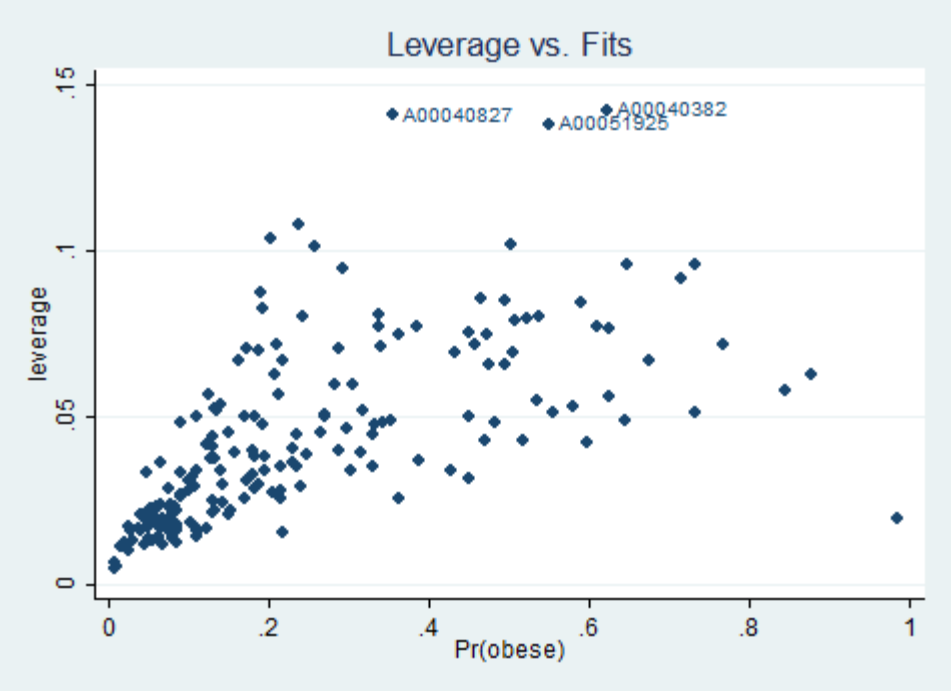

Figure 9. Model Diagnostics: Identifying Covariate Patterns with High Leverage
Illustration of the three covariate patterns exhibiting the highest leverage. In all cases, the flagged subjects had 'middle' values of $\hat{\pi}$, but were not obese.

Most standardized residual values, computed as the change in χ^2 if a given covariate pattern were deleted from the model-building dataset, were low and clustered together ($\Delta\chi^2$<10 for all but four covariate patterns). Four individuals with particularly unusual covariate patterns produced high residual statistics, and were flagged for further examination (see figure below).

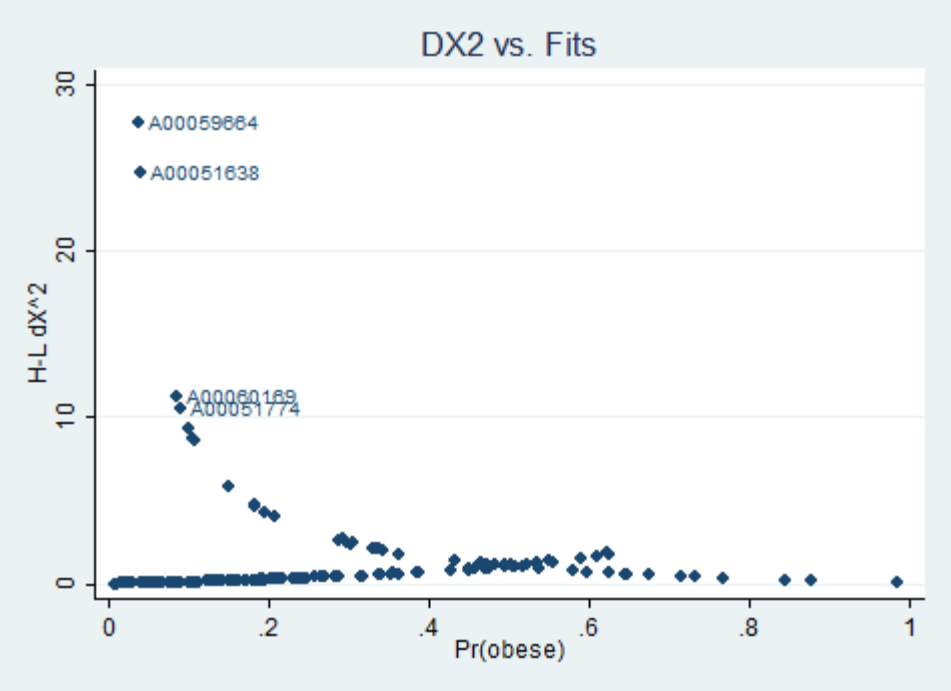

Figure 10. Model Diagnostics: Identifying Covariate Patterns with High Residuals
Illustration of the four covariate patterns exhibiting the highest standardized residuals (computed as the change in $\Delta\chi^2$ if a given covariate pattern was deleted and the model was refit with all but the deleted covariate pattern). In all cases, the flagged subjects were obese but had very small predicted probabilities of being obese (all $\hat{\pi}$ <0.09).

Most covariate patterns had rather low influence on model coefficient estimates ($\Delta\hat{\beta}$<0.6 for all covariate patterns). Only two covariate patterns were associated with $\Delta\hat{\beta}$ influence values that exceeded 0.3. These three individuals were flagged (see figure below).

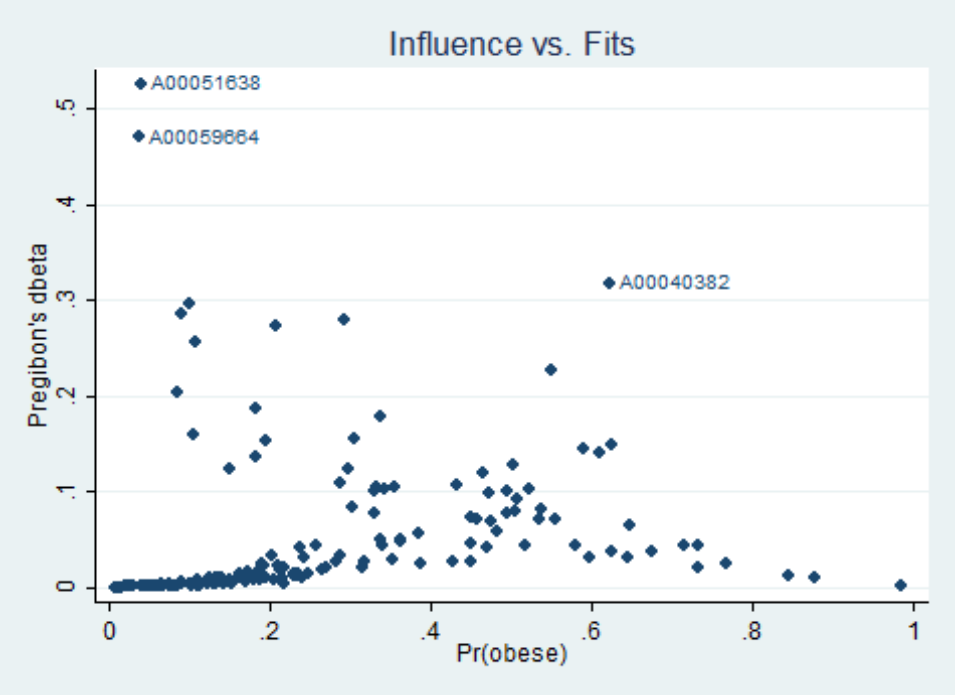

Figure 11. Model Diagnostics: Identifying Covariate Patterns with High Influence
Illustration of the three covariate patterns exhibiting the highest influence on model coefficients (computed as Pregibon's $\Delta\hat{\beta}$ if a given covariate pattern was deleted and the model was refit with all but the deleted covariate pattern). Two cases represent obese individuals predicted to be non-obese, while one case represents a non-obese individual predicted to be obese.

The table below details the effects of removing each of the covariate patterns flagged for high leverage, large standardized residuals, and/or substantial influence on model coefficients; changes in model coefficients which exceed 20% are denoted in bold.

Variable	$\hat{\beta}$ for All Data	Delete A00040382	% change	Delete A00040827	% change	Delete A00051638	% change	Delete A00051774	% change
Constant	5.8260	5.8123	0.24%	5.6919	2.30%	**7.0353**	**20.76%**	5.5287	5.10%
Age (in years)	-0.0566	-0.0483	14.66%	-0.0530	6.36%	**-0.0705**	**24.56%**	-0.0544	3.89%
Inverse Age (in years)	-80.6123	-69.5352	13.74%	-71.5892	11.19%	**-108.9996**	**35.21%**	-79.7687	1.05%
Sex (Female=Referent)	0.9860	1.1339	15.00%	0.9471	3.95%	1.1101	12.59%	0.8891	9.83%
UPPS-P Total Impulsivity Score	0.0324	0.0314	3.09%	0.0332	2.47%	0.0342	5.56%	0.0363	12.04%
Parents' Indexed SES at 16 Years	-0.0375	-0.0390	4.00%	-0.0365	2.67%	-0.0407	8.53%	-0.0407	8.53%
Mean FA – Tract 2 (lOFC ←→ lNAcc)	43.1353	45.0122	4.35%	42.9445	0.44%	47.1114	9.22%	45.5970	5.71%
Mean FA - Tract 3 (lOFC ←→ lIFG)	-48.7592	-51.7152	6.06%	-49.6240	1.77%	-52.0851	6.82%	-51.2537	5.12%
Hosmer-Lemeshow χ^2	8.35	8.65		11.35		11.54		6.88	

Variable	$\hat{\beta}$ for All Data	Delete A00051925	% change	Delete A00059664	% change	Delete A00060169	% change
Constant	5.8260	6.0954	4.62%	5.2335	10.17%	6.5952	13.20%
Age (in years)	-0.0566	-0.0603	6.54%	-0.0593	4.77%	-0.0616	8.83%
Inverse Age (in years)	-80.6123	-88.0889	9.27%	-83.7056	3.84%	-91.7367	13.80%
Sex (Female=Referent)	0.9860	0.9697	1.65%	1.1042	11.99%	1.0531	6.81%
UPPS-P Total Impulsivity Score	0.0324	0.0341	5.25%	0.0348	7.41%	0.0344	6.17%
Parents' Indexed SES at 16 Years	-0.0375	-0.0438	16.80%	-0.0369	1.60%	-0.0383	2.13%
Mean FA – Tract 2 (lOFC ←→ lNAcc)	43.1353	43.1409	0.01%	**52.0034**	**20.56%**	43.5681	1.00%
Mean FA - Tract 3 (lOFC ←→ lIFG)	-48.7592	-48.2673	1.01%	-55.1968	13.20%	-50.4866	3.54%
Hosmer-Lemeshow χ^2	8.35	8.15		6.76		13.46	

Table 7. Effect of Removing Extreme Covariate Patterns

Relevant data detailing the effect of removing each of the seven most extreme covariate patterns iteratively. Removing most covariate patterns results in worse model fit. Few large changes in coefficient estimates were observed (indicated in bold).

While it appears that removing participant A00051638 is associated with a large change in the age coefficients ($\Delta\hat{\beta}$ >20%) and slightly better model discrimination (ΔAUC=0.0192), classification accuracy (Δclassification accuracy = 0.11%) and model fit is better when the covariate pattern associated with this subject is retained [Hosmer-Lemeshow $\chi^2(8)$ = 8.35, p=0.40 for a model with all observations; Hosmer-Lemeshow $\chi^2(8)$ = 11.54, p=0.17 for a model with all observations except A00051638]. Additionally, there does not appear to be a principled reason for excluding this subject from our analyses. This participant ID corresponds to an 18-year-old female with an average impulsivity score, an average parental SES score, an average "reward tract" FA value, and an average "inhibitory tract" FA value. While the model would predict that an observation with these characteristics would be non-obese, this participant happens to be obese.

Additionally, while it appears that removing participant A00059664 is associated with a large change in one of the white matter pathways ($\Delta\hat{\beta}$ = 20.56%), improved model fit [Hosmer-Lemeshow $\chi^2(8)$ = 8.35, p=0.40 for a model with all observations; Hosmer-Lemeshow $\chi^2(8)$ = 6.76, p=0.56 for a model with all observations except A00059664], and better model discrimination (ΔAUC=0.0171), excluding this covariate pattern from the model building dataset results in slightly reduced classification accuracy (Δclassification accuracy = 0.65%). Moreover, there does not appear to be a principled reason for excluding this subject from our analyses. This participant ID corresponds to a 63-year-old female with an average impulsivity score, a lower-than-average parental SES, a lower-than-average "reward tract" FA value, and an average "inhibitory tract" FA

value. While the model would predict that an observation with these characteristics would be non-obese, this participant happens to be obese.

Model Validation

Participants in the holdout sample were classified as obese or non-obese based on the predicted probabilities generated via the final model constructed with the training data, according to a cutoff of 0.27. This cutoff corresponds to the probability value identified within the model building dataset that maximized both sensitivity and specificity. Classification accuracy is represented by the proportion of validation dataset subjects with congruent predicted and observed weight status. Using a 0.27 probability cutoff for obesity and the coefficient estimates produced by the logistic regression model built using the training data, we correctly classified 63.5% of participants. Classifications made using the holdout sample had 72.4% sensitivity (i.e., percentage of subjects classified as obese who were, in fact, obese) and 57.8% specificity (i.e., percentage of subjects classified as non-obese who were, in fact, not obese).

Model Building Dataset					Model Validation Dataset			
	Obese	Non-Obese	Total			Obese	Non-Obese	Total
Classified Obese	33	28	61		Classified Obese	21	19	40
Classified Non-Obese	12	113	125		Classified Non-Obese	8	26	34
Total	45	141	186		Total	29	45	74
Sensitivity = 73.33%		Specificity = 80.14%			Sensitivity = 72.41%		Specificity = 57.78%	
Classification Accuracy = 78.49%					Classification Accuracy = 63.51%			

Table 8. Classification Accuracy: Model Building vs. Model Validation Datasets
Model performance in the training (left panel) and testing (right panel) datasets, including sensitivity, specificity, and overall classification accuracy. Columns indicate true obesity status; rows indicate predicted obesity status.

Importance of Taking a Multi-Disciplinary Approach

An identical model constructed without predictors for white matter integrity underperforms relative to a model that includes brain-derived predictors. A model that excludes parameters for mean fractional anisotropy reduces the area under the ROC curve by 10.5%. Classification accuracy in the model building dataset for a model that omits neuroimaging parameters correctly classifies only 61.7% of participants, relative to 78.5% for a model including these parameters. Sensitivity for a model without imaging parameters is reduced from 73.3% to 60.9% and specificity is reduced from 80.1% to 62.0%.

Similarly, an identical model constructed without predictors for any sociodemographic variables also underperforms relative to a model that includes age, sex, and parents' socioeconomic status during adolescence. A model that excludes parameters for demographic and economic predictors reduces the area under the ROC curve by

5.6%. Classification accuracy in the model building dataset for a model that omits sociodemographic characteristics correctly classifies only 67.4% of participants, relative to 78.5% for a model including these parameters. Sensitivity for a model without sociodemographic predictors is reduced from 73.3% to 66.7% and specificity is reduced from 80.1% to 67.6%.

Discussion

In line with our hypotheses, our results suggest that there may be structural neural correlates of obesity. Using diffusion magnetic resonance imaging, we were able to identify two left-lateralized white matter pathways which, together, provide significant predictive information about obesity status. A connection between the left orbitofrontal cortex and the left inferior frontal gyrus seems to function as an inhibitory-like pathway, such that increased microstructural integrity between these two regions is associated with a decrease in the odds of obesity. This finding builds off of work conducted by Chen and colleagues, who find a similar relationship in chronic dieters between fractional anisotropy in this white matter pathway and percentage body fat (Chen, Chavez, & Heatherton, 2016), which is closely related to obesity status. Interestingly, a connection between the left nucleus accumbens and the orbitofrontal cortex seems to operate as a reward-like pathway, in tandem with the inhibitory pathway. Others have implicated increased frontostriatal microstructural integrity in reward processes [e.g., see (Samanez-Larkin, Levens, Perry, Dougherty, & Knutson, 2012), (Peper, et al., 2013), and (Achterberg, Peper, van Duijvenvoorde, Mandl, & Crone, 2016)]. Given two individuals have similar microstructural integrity within the inhibitory pathway, an increase in the integrity of the reward pathway is associated with an increase in the odds of obesity. As we expected based on prior research [e.g., see (Mobbs, Crepin, Thiery, Golay, & Van der

Linden, 2010), (Jasinska, et al., 2012), and (Sutin, Ferrucci, Zonderman, & Terracciano, 2011)], increases in self-reported impulsive behavior are also associated with an increase in the odds of obesity. Importantly, knowing socioeconomic and demographic characteristics of participants in our sample added to the predictive efficacy of our model. Parents' marital, education, and occupation status when participants were 16-years-old was inversely associated with the odds of obesity, an effect that has been shown in prior studies [e.g., see (Moore, Stunkard, & Srole, 1962)]. Additionally, males were far more likely than females to be obese. This result seems surprising, given that the extant literature does not suggest a strong association between sex and obesity prevalence [in fact, the latest estimates of obesity prevalence among US adults indicate that women experience *higher* obesity prevalence than men (Flegal, Kruszon-Moran, Carroll, Fryar, & Ogden, 2016)]. It is possible that this association is an artifact of the overrepresentation of women in our sample; it is also possible that we are observing a selection effect (e.g., obese women may be less likely to participate in imaging studies). And finally, age was non-linearly associated with obesity such that, in our sample of participants aged 18-85 years, the odds of obesity rose sharply in young adulthood, peaking around 40 years of age, and then began to slowly decline into older age. Again, this is consistent with prior research (Flegal, Kruszon-Moran, Carroll, Fryar, & Ogden, 2016).

Strengths and Limitations

A major strength of this thesis is that, rather than using a typical convenience sample like those that characterize the majority of neuroimaging analyses (Henrich, Heine, & Norenzayan, 2010), we used a dataset collected using population-based sampling methods, including zip-code based recruitment to avoid over-representation of any geographic areas within the target population. Additionally, enrollment was carefully monitored to ensure proportionate representation of sex, race, ethnicity, and socioeconomic status that mirrored 2010 United States census data. Finally, the Rockland Sample utilizes a lifespan approach, which enabled us to get a more complete picture of the odds of obesity throughout adulthood. This thesis attempts to take another small step into the budding field of population neuroscience, which seeks to better characterize social, behavioral, and health outcomes as multi-determined constructs, affected by both the brain and its environment (e.g., parental SES). Our results are likely to be more generalizable than other work conducted in the social neurosciences, especially with respect to populations who represent a range of ages and a diversity of socioeconomic backgrounds. In particular, convenience sampling in typical neuroimaging studies tends to result in the overrepresentation of young, over-educated persons (Henrich, Heine, & Norenzayan, 2010). This suggests that prior neuroimaging studies attempting to describe the personality and neural correlates of obesity may have produced misleading results. For example, in our analyses, restricting observations to college-age persons with above-average parental socioeconomic status (i.e., the "typical" neuroimaging sample) substantively changes the conclusions we might draw from our

model. None of the effects remain significant; if fact, the overall model is no longer significantly different from a model that predicts obesity status without any predictors. The coefficient estimate associated with impulsivity changes by nearly 50%. Though the coefficient estimates for both tracts are remarkably similar in this restricted sample, their standard errors are very large, suggesting that the estimates are unstable and there is a lot of unexplained variability. Thus, it seems clear that taking a lifespan approach with a more representative sample yields meaningfully different results.

This study is not without limitations. Due to time constraints, we were unable to analyze about half of the available data in the Rockland Sample (participants in Releases 1 through 3). Our predictive model would most likely benefit from a larger set of training data, which could have been possible if all imaging data had been preprocessed in time. Additionally, the data analyzed in this thesis are cross-sectional, so we cannot be sure if we have found a neural signature of obesity risk, or rather, if obesity leaves a neural footprint. Also, because our sample only includes adults, we cannot extrapolate our results to children. Given that white matter microstructure, especially in the "reward pathway" investigated, matures during childhood and adolescence (Mills, Goddings, Clasen, Giedd, & Blakemore, 2014), age would likely need to be re-parameterized to predict obesity status in a sample that included both children and adults.

Future Directions

Though this thesis only utilizes the data from the Cross-Sectional Lifespan Connectomics Study arm of the Rockland Sample, future work could begin to tackle the question of whether the integrity of our "reward" and "inhibitory" white matter pathways is a cause or consequence of obesity. The Rockland Sample includes two longitudinal study arms – the Longitudinal Developmental Connectomics Study (which samples children aged 6 to 17.9 years at enrollment and follows them for three waves of data collection separated by 15-month intervals) and the Adult Longitudinal Study [a newly funded study arm that will follow adults aged 38-71.9 years for a period of 4 years (data have not yet been released)]. These longitudinal samples might be used in future studies to predict incident, rather than prevalent, obesity using similar measures of white matter integrity explored in this thesis.

An additional point of inquiry worth pursuing might be to investigate whether these white matter pathways confer a specific risk of obesity, or whether they are a general biomarker for engaging in unhealthy behaviors that tend to favor immediate gratification over long-term rewards. It is highly unlikely that there are entire neural pathways devoted to rewarding overindulgence in food and/or inhibiting impulses to engage in overeating. It is far more likely that the pathways identified in this thesis serve more general reward-seeking and inhibitory functions. Future work could investigate whether similar microstructural integrity is implicated in predicting the odds of being a current smoker, an alcoholic, a drug addict, a chronic video-gamer, a gambler, etc. In

fact, it may be possible to use the model built for this thesis as a foundation for a building a more complex multinomial logistic regression model that predicts to which self-regulatory failure, in particular, an individual may be susceptible.

Public Health Relevance

This thesis serves as a first step in characterizing the normal variability in brain microstructure over the lifespan, as it pertains to health outcomes. In particular, we attempt to map the adult developmental trajectory of normal and at-risk neural structure by using deviations from the neural norm in two white matter pathways to predict obesity status. Furthermore, by including relevant social predictors, like parental education and occupation status during childhood, we have begun the difficult task of characterizing the distribution of brain structure at the population-level, unconfounded by some exposures at the societal level.

Though a somewhat distant goal, there are also potential public health implications of this thesis for individualized, preventative healthcare (Paus, 2013). If white matter microstructure in the "reward" and "inhibitory" tracts identified in this thesis are shown to be a neural biomarker for future risky decision-making related to poor health outcomes (e.g., smoking initiation, binge drinking, overeating, etc.), the eventual implications of this line of research are that we will be able to diagnose vulnerability to obesity, addiction, and their associated health risks before individuals engage in risk behaviors. This would allow us to develop targeted intervention and prevention

approaches by incorporating neural endophenotypes of risk in our predictive models. In particular, if these risk profiles could be explicated in children, we could exploit our knowledge of plasticity in white matter development to alter the trajectory of microstructural integrity in these tracts, thereby reducing incidence of addictive behaviors and disorders in the future.

Conclusions

Inhibitory and reward pathways in the brain work in concert to predict obesity status. These relationships are qualified by sex, age, and parental socioeconomic status during childhood. Population neuroscience can be usefully applied toward a more nuanced understanding of chronic disease and negative health behaviors.

References

Achterberg, M., Peper, J. S., van Duijvenvoorde, A. K., Mandl, R. W., & Crone, E. A. (2016). Frontostriatal white matter integrity predicts development of delay of gratification: a longitudinal study. *The Journal of Neuroscience*, 36(6):1954-1961.

Ainslie, G. (1975). Specious reward: a behavioral theory of impulsiveness and impulse control. *Psychological Bulletin*, 82(4):463-496.

Baker, J. L., Olsen, L. W., & Sorensen, T. I. (2007). Child body-mass index and the risk of coronary heart disease in adulthood. *The New England Journal of Medicine*, 357:2329-2337.

Basser, P. J., & Pierpaoli, C. (1996). Microstructural and physiological features of tissues elucidated by quantitative-diffusion-tensor MRI. *Journal of Magnetic Resonance*, Series B 111:209-219.

Behrens, T. J., Berg, H. J., Jbabdi, S., Rushworth, M. S., & Woolrich, M. W. (2007). Probabilistic diffusion tractography with multiple fibre orientations: what can we gain? *NeuroImage*, 34(1):144-155.

Behrens, T. J., Woolrich, M. W., Jenkinson, M., Johansen-Berg, H., Nunes, R. G., Clare, S., Matthews, P. M., Brady, J. M., & Smith, S. M. (2003). Characterization and propagation of uncertainty in diffusion-weighted MR imaging. *Magnetic Resonance in Medicine*, 50(5):1077-1088.

Berkman, E. T., & Falk, E. B. (2013). Beyond brain mapping: using neural measures to predict real-world outcomes. *Current Directions in Psychological Science*, 22(1):45-50.

Blakemore, S.-J., & Choudhury, S. (2006). Development of the adolescent brain: implications for executive function and social cognition. *Journal of Child Psychology and Psychiatry*, 47(3/4):296-312.

Cacioppo, J. T., Berntson, G. G., Sheridan, J. F., & McClintock, M. K. (2000). Multilevel integrative analyses of human behavior: social neuroscience and the complementing nature of social and biological approaches. *Psychological Bulletin*, 126(6):829-843.

Calle, E. E., Rodriguez, C., Walker-Thurmond, K., & Thun, M. J. (2003). Overweight, obesity, and mortality from cancer in a prospectively studied cohort of U.S. adults. *The New England Journal of Medicine*, 348:1625-1638.

Cappuccio, F. P., Taggart, F. M., Kandala, N.-B., Currie, A., Peile, E., Stranges, S., & Miller, M. A. (2008). Meta-analysis of short sleep duration and obesity in children and adults. *Sleep*, 31(5):619-626.

Chen, P.-H. A., Chavez, R. S., & Heatherton, T. F. (2016). Structural integrity between executive control and reward regions of the brain predicts body fat percentage in chronic dieters. *Cognitive Neuroscience*, DOI: 10.1080/17588928.2016.1235556.

Coultee, C. G., & Huettel, S. A. (2012). The functional neuroanatomy of decision making: prefrontal control of thought and action. *Brain Research*, 1428C:3-12.

Cross, C. P., Copping, L. T., & Cambell, A. (2011). Sex differences in impulsivity: a meta-analysis. *Psychological Bulletin*, 137(1):97-130.

Emsell, L., Van Hecke, W., & Tournier, J.-D. (2016). Introduction to Diffusion Tensor Imaging. In L. Emsell, W. Van Hecke, & J.-D. Tournier, *Diffusion Tensor Imaging: A Practical Handbook* (pp. 7-19). New York: Springer.

Falk, E. B., Hyde, L. W., Mitchell, C., Faul, J., Gonzalez, R., Heitzeg, M. M., Keating, D. P., Langa, K. M., Martz, M. E., Maslowsky, J., Morrison, F. J., Noll, D. C., Patrick, M. E., Pfeffer, F. T., Reuter-Lorenz, P. A., Thomason, M. E., Davis-Kean, P., Monk, C. S., & Schulenberg, J. (2013). What is a representative brain? Neuroscience meets population science. *Proceedings of the National Academy of Sciences*, 110(44):17615-22.

Feinberg, D. A., & Setsompop, K. (2013). Ultra-fast MRI of the human brain with simultaneous multi-slice imaging. *Journal of Magnetic Resonance*, 229:90-100.

Flegal, K. M., Carroll, M. D., Kit, B. K., & Ogden, C. L. (2012). Prevalence of obesity and trends in the distribution of body mass index among US adults, 1999-2010. *The Journal of the American Medical Association*, 307(5):491-497.

Flegal, K. M., Kruszon-Moran, D., Carroll, M. D., Fryar, C. D., & Ogden, C. L. (2016). Trends in obesity among adults in the United States, 2005 to 2014. *The Journal of the American Medical Association*, 315(21):2284-91.

Gianaros, P. J., Horenstein, J. A., Hariri, A. R., Sheu, L. K., Manuck, S. B., Matthews, K. A., & Cohen, S. (2008). Potential neural embedding of parental social standing. *Social Cognitive and Affective Neuroscience*, 3(2):91-96.

Gianaros, P. J., Manuck, S. B., Sheu, L. K., Kuan, D. C., Votruba-Drzal, E., Craig, A. E., & Hariri, A. R. (2011). Parental education predicts corticostriatal functionality in adulthood. *Cerebral Cortex*, 21(4):896-910.

Gianaros, P. J., Marsland, A. L., Sheu, L. K., Erickson, K. I., & Verstynen, T. D. (2013). Inflammatory pathways link socioeconomic inequalities to white matter architecture. *Cerebral Cortex*, 23(9):2058-2071.

Gironda, R. J., Lloyd, J., Clark, M. E., & Walker, R. L. (2007). Preliminary evaluation of reliability and criterion validity of actiwatch-score. *Journal of Rehabilitation Research and Development*, 44(2):223-30.

Grandner, M. A., Schopfer, E. A., Sands-Lincoln, M., Jackson, N., & Malhotra, A. (2015). Relationship between sleep duration and body mass index depends on age. *Obesity (Silver Spring)*, 23(12):2491-2498.

Guh, D. P., Zhang, W., Bansback, N., Amarsi, Z., Birmingham, C. L., & Anis, A. H. (2009). The incidence of co-morbidities related to obesity and overweight: a systematic review and meta-analysis. *BMC Public Health*, 9(88).

Haas, J. S., Lee, L. B., Kaplan, C. P., Sonneborn, D., Phillips, K. A., & Liang, S.-Y. (2003). The association of race, socioeconomic status, and health insurance status with the prevalence of overweight among children and adolescents. *American Journal of Public Health*, 93:2105-2110.

Hariri, A. R. (2009). The neurobiology of individual differences in complex behavioral traits. *Annual Review of Neuroscience*, 32:225-247.

Heatherton, T. F., & Wagner, D. D. (2011). Cognitive neuroscience of self-regulation failure. *Trends in Cognitive Sciences*, 15(3):132-139.

Henrich, J., Heine, S. J., & Norenzayan, A. (2010). The weirdest people in the world? *Behavioral and Brain Sciences*, 33:61-135.

Hibar, D. P., Stein, J. L., Renteria, M. E., Arias-Vasquez, A., Desrivieres, S., Jahanshad, N., Toro, R., Wittfeld, K., Abramovic, L., Andersson, M., Aribisala, B. S., Armstrong, N. J., Bernard, M., Bohlken, M. M., Boks, M. P., Bralten, J., Brown, A. A., Chakravarty, M. M., Chen, Q., Ching, C. R. K., Cuellar-Partida, G., den Braber, A., Giddaluru, S., Goldman, A. L., Grimm, O., Guadalupe, T., Hass, J., Woldehawariat, G., Holmes, A. J., Hoogman, M., Janowitz, D., Jia, T., Kim, S., Klein, M., Kraemer, B., Lee, P. H., Olde Loohuis, L. M., Luciano, M., Macare, C., Mather, K. A., Mattheisen, M., Milaneschi, Y., Nho, K., Papmeyer, M., Ramasamy, A., Risacher, S. L., Roiz-Santiañez, R., Rose, E. J., Salami, A., Sämann, P. G., Schmaal, L., Schork, A. J., Shin, J., Strike, L. T., Teumer, A., van Donkelaar, M. M. J., van Eijk, K. R., Walters, R. K., Westlye, L. T., Whelan, C. D., Winkler, A. M., Zwiers, M. P., Alhusaini, S., Athanasiu, L., Ehrlich, S., Hakobjan, M. M. H., Hartberg, C. B., Haukvik, U. K., Heister, A. J. G. A. M., Hoehn, D., Kasperaviciute, D., Liewald, D. C. M., Lopez, L. M., Makkinie, R. R. R., Matarin, M., Naber, M. A. M., McKay, D. R., Needham, M., Nugent, A. C., Pütz, B., Royle, N. A., Shen, L., Sprooten, E., Trabzuni, D., van der Marel, S. S.

L., van Hulzen, K. J. E., Walton, E., Wolf, C., Almasy, L., Ames, D., Arepalli, S., Assareh, A. A., Bastin, M. E., Brodaty, H., Bulayeva, K. B., Carless, M. A., Cichon, S., Corvin, A., Curran, J. E., Czisch, M., de Zubicaray, G. I., Dillman, A., Duggirala, R., Dyer, T. D., Erk, S., Fedko, I. O., Ferrucci, L., Foroud, T. M., Fox, P. T., Fukunaga, M., Gibbs, J. R., Göring, H. H. H., Green, R. C., Guelfi, S., Hansell, N. K., Hartman, C. A., Hegenscheid, K., Heinz, A., Hernandez, D. G., Heslenfeld, D. J., Hoekstra, P. J., Holsboer, F., Homuth, G., Hottenga, J-J., Ikeda, M., Jack, C. R., Jr., Jenkinson, M., Johnson, R., Kanai, R., Keil, M., Kent, J. W., Jr., Kochunov, P., Kwok, J. B., Lawrie, S. M., Liu, X., Longo, D. L., McMahon, K. L., Meisenzahl, E., Melle, I., Mohnke, S., Montgomery, G. W., Mostert, J. C., Mühleisen, T. W., Nalls, M. A., Nichols, T. E., Nilsson, L. G., Nöthen, M. M., Ohi, K., Olvera, R. L., Perez-Iglesias, R., Pike, G. B., Potkin, S. G., Reinvang, I., Reppermund, S., Rietschel, M., Romanczuk-Seiferth, N., Rosen, G. D., Rujescu, D., Schnell, K., Schofield, P. R., Smith, C., Steen, V. M., Sussmann, J. E., Thalamuthu, A., Toga, A. W., Traynor, B. J., Troncoso, J., Turner, J. A., Valdés-Hernández, M. C., van 't Ent, D., van der Brug, M., van der Wee, N. J. A., van Tol, M-J., Veltman, D. J., Wassink, T. H., Westman, E., Zielke, R. H., Zonderman, A. B., Ashbrook, D. G., Hager, R., Lu, L., McMahon, F. J., Morris, D. W., Williams, R. W., Brunner, H. G., Buckner, R. L., Buitelaar, J. K., Cahn, W., Calhoun, V. D., Cavalleri, G. L., Crespo-Facorro, B., Dale, A. M., Davies, G. E., Delanty, N., Depondt, C., Djurovic, S., Drevets, W. C., Espeseth, T., Gollub, R. L., Ho, B-C., Hoffmann, W., Hosten, N., Kahn, R. S., Le Hellard, S., Meyer-Lindenberg, A., Müller-Myhsok, B., Nauck, M., Nyberg, L., Pandolfo, M., Penninx, B. W. J. H., Roffman, J. L., Sisodiya, S. M., Smoller, J. W., van Bokhoven, H., van Haren, N. E. M., Völzke, H., Walter, H., Weiner, M. W., Wen, W., White, T., Agartz, I., Andreassen, O. A., Blangero, J., Boomsma, D. I., Brouwer, R. M., Cannon, D. M., Cookson, M. R., de Geus, E. J. C., Deary, I. J., Donohoe, G., Fernández, G., Fisher, S. E., Francks, C., Glahn, D. C., Grabe, H. J., Gruber, O., Hardy, J., Hashimoto, R., Hulshoff Pol, H. E., Jönsson, E. G., Kloszewska, I., Lovestone, S., Mattay, V. S., Mecocci, P., McDonald, C., McIntosh, A. M., Ophoff, R. A., Paus, T., Pausova, Z., Ryten, M., Sachdev, P. S., Saykin, A. J., Simmons, A., Singleton, A., Soininen, H., Wardlaw, J. M., Weale, M. E., Weinberger, D. R., Adams, H. H. H., Launer, L. J., Seiler, S., Schmidt, R., Chauhan, G., Satizabal, C. L., Becker, J. T., Yanek, L., van der Lee, S. J., Ebling, M., Fischl, B., Longstreth, W. T., Jr., Greve, D., Schmidt, H., Nyquist, P., Vinke, L. N., van Duijn, C. M., Xue, L., Mazoyer, B., Bis, J. C., Gudnason, V., Seshadri, S., Ikram, M. A., The Alzheimer's Disease Neuroimaging Initiative, The CHARGE Consortium, EPIGEN, IMAGEN, SYS, Martin, N. G., Wright, M. J., Schumann, G., Franke, B., Thompson, P. M., & Medland, S. E. (2015). Common genetic variants influence human subcortical brain structures. *Nature*, 520(7546):224-229.

Hollingshead, A. B. (1975). Four-factor index of social status. *Unpublished manuscript*, 651662.

Hosmer, D. W., & Lemeshow, S. (2000). *Applied Logistic Regression. 2nd ed*. New York, NY: John Wiley & Sons, Inc.

Hsu, F.-C., Yuan, M., Bowden, D. W., Xu, J., Smith, S. C., Wagenknecht, L. E., Langefeld, C. D., Divers, J., Register, T. C., Carr, J. J., Williamson, J. D., Sink, K. M., Maldjian, J. A., & Freedman, B. I. (2016). Adiposity is inversely associated with hippocampal volume in African Americans and European Americans with diabetes. *Journal of Diabetes and its Complications*, 30(8):1506-1512.

Jasinska, A. J., Yasuda, M., Burant, C. F., Gregor, N., Khatri, S., Sweet, M., & Falk, E. B. (2012). Impulsivity and inhibitory control deficits are associated with unhealthy eating in young adults. *Appetite*, 59(3):738-747.

Jednorog, K., Altarelli, I., Monzalvo, K., Fluss, J., Dubois, J., Billard, C., Dehaene-Lambertz, G., & Ramus, F. (2012). The influence of socioeconomic status on children's brain structure. *PLOS ONE*, 7(10).

Jenkinson, M., Bannister, P., Brady, M., & Smith, S. (2002). Improved optimization for the robust and accurate linear registration and motion correction of brain images. *NeuroImage*, 17:825-841.

Johnson, S. L., Turner, R. J., & Iwata, N. (2003). BIS/BAS levels and psychiatric disorder: an epidemiological study. *Journal of Psychopathology and Behavioral Assessment*, 25(1):25-36.

Klein, S., Burke, L. E., Bray, G. A., Blair, S., Allison, D. B., Pi-Sunyer, X., Hong, Y., & Eckel, R. H. (2004). Clinical implications of obesity with specific focus on cardiovascular disease. *Circulation*, 110:2952-2967.

Kober, H., Mende-Siedlecki, P., Kross, E. F., Weber, J., Mischel, W., Hart, C. L., & Ochsner, K. N. (2010). Prefrontal-striatal pathway underlies cognitive regulation of craving. *Proceedings of the National Academy of Sciences*, 107(33):14811-14816.

Kochunov, P., Williamson, D. E., Lancaster, J., Fox, P., Cornell, J., Blangero, J., & Glahn, D. C. (2012). Fractional anisotropy of water diffusion in cerebral white matter across the lifespan. *Neurobiology of Aging*, 33(1):9-20.

Kottke, T. E., Wu, L. A., & Hoffman, R. S. (2003). Economic and psychological implications of the obesity epidemic. *Mayo Clinical Proceedings*, 78:92-94.

Kringelbach, M. L. (2005). The human orbitofrontal cortex: linking reward to hedonic experience. *Nature Reviews*, 6:691-702.

Kullmann, S., Schweizer, F., Veit, R., Fritsche, A., & Preissl, H. (2015). Compromised white matter integrity in obesity. *Obesity Reviews*, 16(4):273-281.

Lantz, P. M., House, J. S., Lepkowski, J. M., Williams, D. R., Mero, R. P., & Chen, J. (1998). Socioeconomic factors, health behaviors, and mortality: results from a nationally representative prospective study of US adults. *Journal of the American Medical Association*, 279(21):1703-1708.

Lawrence, A. J., Luty, J., Bogdan, N. A., Sahakian, B. J., & Clark, L. (2009). Impulsivity and response inhibition in alcohol dependence and problem gambling. *Psychopharmacology*, 207(1):163-172.

Le Bihan, D., Mangin, J.-F., Poupon, C., Clark, C. A., Pappata, S., Molko, N., & Chabriat, H. (2001). Diffusion tensor imaging: concepts and applications. *Journal of Magnetic Resonance Imaging*, 13(4):534-546.

Lebel, C., Gee, M., Camicioli, R., Wieler, M., Martin, W., & Beaulieu, C. (2012). Diffusion tensor imaging of white matter tract evolution over the lifespan. *NeuroImage*, 60(1):340-352.

Logan, G. D., Schachar, R. J., & Tannock, R. (1997). Impulsivity and inhibitory control. *Psychological Science*, 8(1):60-64.

Marqués-Iturria, I., Scholtens, L. H., Garolera, M., Pueyo, R., García-García, I., González-Tartiere, P., Segura, B., Junqué, C., Sender-Palacios, M. J., Vernet-Vernet, M., Sánchez-Garre, C., de Reus, M. A., Jurado, M. A., & van den Heuvel, M. P. (2015). Affected connectivity organization of the reward system structure in obesity. *NeuroImage*, 111:100-106.

Mills, K. L., Goddings, A. L., Clasen, L. S., Giedd, J. N., & Blakemore, S. J. (2014). The developmental mismatch in structural brain maturation during adolescence. *Developmental Neuroscience*, 36:147-160.

Mischel, W. (1974). Processes in delay of gratification. *Advances in Experimental Social Psychology*, 7:249-292.

Mischel, W., Ebbesen, E. B., & Raskoff Zeiss, A. (1972). Cognitive and attentional mechanisms in delay of gratification. *Journal of Personality and Social Psychology*, 21(2):204-218.

Mischel, W., Shoda, Y., & Rodriguez, M. L. (1989). Delay of gratification in children. *Science*, 244(4907):933-938.

Mobbs, O., Crepin, C., Thiery, C., Golay, A., & Van der Linden, M. (2010). Obesity and the four facets of impulsivity. *Patient Education and Counseling*, 79(3):372-377.

Moore, M. E., Stunkard, A., & Srole, L. (1962). Obesity, social class, and mental illness. *Journal of the American Medical Association*, 181(11):962-966.

Nederkoorn, C., Braet, C., Van Eijs, Y., Tanghe, A., & Jansen, A. (2006). Why obese children cannot resist food: the role of impulsivity. *Eating Behaviors*, 7:315-322.

Noble, K. G., Houston, S. M., Kan, E., & Sowell, E. R. (2012). Neural correlates of socioeconomic status in the developing human brain. *Developmental Science*, 1-12.

Noble, K. G., Wolmetz, M. E., Ochs, L. G., Farah, M. J., & McCandliss, B. D. (2006). Brain-behavior relationships in reading acquisition are modulated by socioeconomic factors. *Developmental Science*, 9(6):642-654.

Nooner, K. B., Colcombe, S. J., Tobe, R. H., Mennes, M., Benedict, M. M., Moreno, A. L., Panek, L. J., Brown, S., Zavitz, S. T., Li, Q., Sikka, S., Gutman, D., Bangaru, S., Schlachter, R. T., Kamiel, S. M., Anwar, A. R., Hinz, C. M., Kaplan, M. S., Rachlin, A. B., Adelsberg, S., Cheung, B., Khanuja, R., Yan, C., Craddock, C. C., Calhoun, V., Courtney, W., King, M., Wood, D., Cox, C. L., Kelly, A. M. C., Di Martino, A., Petkova, E., Reiss, P. T., Duan, N., Thomsen, D., Biswal, B., Coffey, B., Hoptman, M. J., Javitt, D. C., Pomara, N., Sidtis, J. J., Koplewicz, H. S., Castellanos, F. X., Leventhal, B. L., & Milham, M. P. (2012). The NKI-Rockland sample: a model for accelerating the pace of discovery science in psychiatry. *Frontiers in Neuroscience*, 6:152.

Ogden, C. L., Carroll, M. D., Kit, B. K., & Flegal, K. M. (2014). Prevalence of childhood and adult obesity in the United States, 2011-2012. *Journal of the American Medical Association*, 311(8):806-814.

Olson, E. A., Collins, P. F., Hooper, C. J., Muetzel, R., Lim, K. O., & Luciana, M. (2009). White matter integrity predicts delay discounting behavior in 9- to 23-year-olds: a diffusion tensor imaging study. *Journal of Cognitive Neuroscience*, 21(7):1406-1421.

Patel, S. R., & Hu, F. B. (2008). Short sleep duration and weight gain: a systematic review. *Obesity*, 16(3):643-653.

Patenaude, B., Smith, S. M., Kennedy, D., & Jenkinson, M. A. (2011). A Bayesian model of shape and appearance for subcortical brain segmentation. *NeuroImage*, 56(3):907-922.

Paus, T. (2013). *Population Neuroscience*. Springer Science & Business Media.

Peper, J. S., Mandl, R. C., Braams, B. R., de Water, E., Heijboer, A. C., Koolschijn, P. C., & Crone, E. A. (2013). Delay discounting and frontostriatal fiber tracts: a combined DTI and MTR study on impulsive choices in healthy young adults. *Cerebral Cortex*, 23(7):1695-1702.

Pregibon, D. (1981). Logistic regression diagnostics. *The Annals of Statistics*, 9(4):705-724.

Puhl, R. M., & Heuer, C. A. (2009). The stigma of obesity: a review and update. *Obesity*, 17(5):941-964.

Raizada, R. D., Richards, T. L., Meltzoff, A., & Kuhl, P. K. (2008). Socioeconomic status predicts hemispheric specialization of the left inferior frontal gyrus in young children. *NeuroImage*, 40:1392-1401.

Ryb, G. E., Dischinger, P. C., Kufera, J. A., & Read, K. M. (2006). Risk perception and impulsivity: association with risky behavior and substance abuse disorders. *Accident Analysis & Prevention*, 38(3):567-573.

Salgado, J. F. (2002). The big five personality dimensions and counterproductive behaviors. *International Journal of Selection and Assessment*, 10(1/2):117-125.

Samanez-Larkin, G. R., & Knutson, B. (2015). Decision making in the ageing brain: changes in affective and motivational circuits. *Nature Reviews*, 16:278-289.

Samanez-Larkin, G. R., Levens, S. M., Perry, L. M., Dougherty, R. F., & Knutson, B. (2012). Frontostriatal white matter integrity mediates adult age differences in probabilistic reward learning. *The Journal of Neuroscience*, 32(15):5333-5337.

Schlam, T. R., Wilson, N. L., Shoda, Y., Mischel, W., & Ayduk, O. (2013). Preschoolers' delay of gratification predicts their body mass 30 years later. *Journal of Pediatrics*, 162(1):90-93.

Scott, A., Courtney, W., Wood, D., de la Garza, R., Lane, S., King, M., Wang, R., Roberts, J., Turner, J. A., & Calhoun, V. D. (2011). COINS: an innovative informatics and neuroimaging tool suite built for large heterogeneous datasets. *Frontiers in Neuroinformatics*, 5:33.

Simmonds, D. J., Hallquist, M. N., Asato, M., & Luna, B. (2014). Developmental stages and sex differences of white matter and behavioral development through adolescence: a longitudinal diffusion tensor imaging (DTI) study. *NeuroImage*, 92:356-368.

Sobal, J., & Stunkard, A. J. (1989). Socioeconomic status and obesity: a review of the literature. *Psychological Bulletin*, 105(2):260-275.

Somerville, L. H., Jones, R. M., & Casey, B. J. (2010). A time of change: behavioral and neural correlates of adolescent sensitivity to appetitive and aversive environmental cues. *Brain and Cognition*, 72(1):124-133.

Sowell, E. R., Peterson, B. S., Thompson, P. M., Welcome, S. E., Henkenius, A. L., & Toga, A. W. (2003). Mapping cortical change across the human life span. *Nature Neuroscience*, 6:309-315.

Spieker, E. A., & Pyzocha, N. (2016). Economic impact of obesity. *Primary Care: Clinics in Office Practice*, 43(1):83-95.

Steinberg, L. (2008). A social neuroscience perspective on adolescent risk-taking. *Developmental Review*, 28(1):78-106.

Steinberg, L., Albert, D., Cauffman, E., Banich, M., Graham, S., & Woolard, J. (2008). Age differences in sensation seeking and impulsivity as indexed by behavior and self-report: evidence for a dual systems model. *Developmental Psychology*, 44(6):1764-1778.

Strauss, R. S., & Pollack, H. A. (2003). Social marginalization of overweight children. *Archives of Pediatrics and Adolescent Medicine*, 157:746-752.

Sutin, A. R., Ferrucci, L., Zonderman, A. B., & Terracciano, A. (2011). Personality and obesity across the adult lifespan. *Journal of Personality and Social Psychology*, 101(3):579-592.

Taki, Y., & Kawashima, R. (2012). Brain development in childhood. *The Open Neuroimaging Journal*, 6:103-110.

Telzer, E. H., Fuligni, A. J., Lieberman, M. D., & Galvan, A. (2013). The effects of poor sleep quality on brain function and risk taking in adolescence. *NeuroImage*, 71:275-283.

Telzer, E. H., Goldenberg, D., Fuligini, A. J., Lieberman, M. D., & Galvan, A. (2015). Sleep variability in adolescence is associated with altered brain development. *Developmental Cognitive Neuroscience*, 14:16-22.

Tomasi, D., & Volkow, N. D. (2013). Striatocortical pathway dysfunction in addiction and obesity: differences and similarities. *Critical Reviews in Biochemistry and Molecular Biology*, 48(1):1-19.

U.S. Census Bureau. (2015). U.S. Census Bureau State & County Quickfacts: U.S.A. *Available at: https://www.census.gov/quickfacts/table/PST045215/36087,00*, [accessed October 7, 2016].

Uchino, B. N. (2006). Social support and health: a review of physiological processes potentially underlying links to disease outcomes. *Journal of Behavioral Medicine*, 29(4):377-387.

Verdejo-Garcia, A., Lawrence, A. J., & Clark, L. (2008). Impulsivity as a vulnerability marker for substance-use disorders: review of findings from high-risk research, problem gamblers and genetic association studies. *Neuroscience and Biobehavioral Reviews*, 32(4):777-810.

Vink, M., Kleerekooper, I., van den Wildenberg, W. P., & Kahn, R. S. (2015). Impact of aging on frontostriatal reward processing. *Human Brain Mapping*, 36(6):2305-2317.

Whiteside, S. P., & Lynham, D. R. (2001). The Five Factor Model and impulsivity: using a structural model of personality to understand impulsivity. *Personality and Individual Differences*, 30(4):669-689.

Whiteside, S. P., Lynam, D. R., Miller, J. D., & Reynolds, S. K. (2005). Validation of the UPPS impulsive behaviour scale: a four-factor model of impulsivity. *European Journal of Personality*, 19:559-574.

Williams, D. R., & Collins, C. (2001). Racial residential segregation: a fundamental cause of racial disparities in health. *Public Health Reports*, 116:404-416.

Winkelman, J. W., Benson, K. L., Buxton, O. M., Lyoo, I. K., Yoon, S., O'Connor, S., & Renshaw, P. F. (2010). Lack of hippocampal volume differences in primary insomnia and good sleeper controls: an MRI volumetric study at 3 Tesla. *Sleep Medicine*, 11(6):576-582.

Winker, M. A. (2004). Measuring race and ethnicity: Why and how? *Journal of the American Medical Association*, 292(13):1612-1614.

World Health Organization. (2000). Obesity: preventing and managing the global epidemic. Report of a WHO consultation on obesity. *WHO Technical Report Series*, 894.

Yarkoni, T., Poldrack, R. A., Nichols, T. E., Van Essen, D. C., & Wager, T. D. (2011). Large-scale automated synthesis of human functional neuroimaging data. *Nature Methods*, 8(8):665-674.

Appendix A: UPPS-P

UPPS-P

Below are a number of statements that describe ways in which people act and think. For each statement, please indicate how much you agree or disagree with the statement. If you **Agree Strongly** circle **1**, if you **Agree Somewhat** circle **2**, if you **Disagree somewhat** circle **3**, and if you **Disagree Strongly** circle **4**. Be sure to indicate your agreement or disagreement for every statement below. Also, there are questions on the following pages.

	Agree Strongly	Agree Some	Disagree Some	Disagree Strongly
1. I have a reserved and cautious attitude toward life.	1	2	3	4
2. I have trouble controlling my impulses.	1	2	3	4
3. I generally seek new and exciting experiences and sensations.	1	2	3	4
4. I generally like to see things through to the end.	1	2	3	4
5. When I am very happy, I can't seem to stop myself from doing things that can have bad consequences.	1	2	3	4
6. My thinking is usually careful and purposeful.	1	2	3	4
7. I have trouble resisting my cravings (for food, cigarettes, etc.).	1	2	3	4
8. I'll try anything once.	1	2	3	4
9. I tend to give up easily.	1	2	3	4
10. When I am in great mood, I tend to get into situations that could cause me problems.	1	2	3	4
11. I am not one of those people who blurt out things without thinking.	1	2	3	4
12. I often get involved in things I later wish I could get out of.	1	2	3	4
13. I like sports and games in which you have to choose your next move very quickly.	1	2	3	4
14. Unfinished tasks really bother me.	1	2	3	4
15. When I am very happy, I tend to do things that may cause problems in my life.	1	2	3	4
16. I like to stop and think things over before I do them.	1	2	3	4
17. When I feel bad, I will often do things I later regret in order to make myself feel better now.	1	2	3	4
18. I would enjoy water skiing.	1	2	3	4
19. Once I get going on something I hate to stop.	1	2	3	4
20. I tend to lose control when I am in a great mood.	1	2	3	4
21. I don't like to start a project until I know exactly how to proceed.	1	2	3	4

Please go to the next page

	Agree Strongly	Agree Some	Disagree Some	Disagree Strongly
22. Sometimes when I feel bad, I can't seem to stop what I am doing even though it is making me feel worse.	1	2	3	4
23. I quite enjoy taking risks.	1	2	3	4
24. I concentrate easily.	1	2	3	4
25. When I am really ecstatic, I tend to get out of control.	1	2	3	4
26. I would enjoy parachute jumping.	1	2	3	4
27. I finish what I start.	1	2	3	4
28. I tend to value and follow a rational, "sensible" approach to things.	1	2	3	4
29. When I am upset I often act without thinking.	1	2	3	4
30. Others would say I make bad choices when I am extremely happy about something.	1	2	3	4
31. I welcome new and exciting experiences and sensations, even if they are a little frightening and unconventional.	1	2	3	4
32. I am able to pace myself so as to get things done on time.	1	2	3	4
33. I usually make up my mind through careful reasoning.	1	2	3	4
34. When I feel rejected, I will often say things that I later regret.	1	2	3	4
35. Others are shocked or worried about the things I do when I am feeling very excited.	1	2	3	4
36. I would like to learn to fly an airplane.	1	2	3	4
37. I am a person who always gets the job done.	1	2	3	4
38. I am a cautious person.	1	2	3	4
39. It is hard for me to resist acting on my feelings.	1	2	3	4
40. When I get really happy about something, I tend to do things that can have bad consequences.	1	2	3	4
41. I sometimes like doing things that are a bit frightening.	1	2	3	4
42. I almost always finish projects that I start.	1	2	3	4
43. Before I get into a new situation I like to find out what to expect from it.	1	2	3	4
44. I often make matters worse because I act without thinking when I am upset.	1	2	3	4
45. When overjoyed, I feel like I can't stop myself from going overboard.	1	2	3	4

Please go to the next page

	Agree Strongly	Agree Some	Disagree Some	Disagree Strongly
46. I would enjoy the sensation of skiing very fast down a high mountain slope.	1	2	3	4
47. Sometimes there are so many little things to be done that I just ignore them all.	1	2	3	4
48. I usually think carefully before doing anything.	1	2	3	4
49. When I am really excited, I tend not to think of the consequences of my actions.	1	2	3	4
50. In the heat of an argument, I will often say things that I later regret.	1	2	3	4
51. I would like to go scuba diving.	1	2	3	4
52. I tend to act without thinking when I am really excited.	1	2	3	4
53. I always keep my feelings under control.	1	2	3	4
54. When I am really happy, I often find myself in situations that I normally wouldn't be comfortable with.	1	2	3	4
55. Before making up my mind, I consider all the advantages and disadvantages.	1	2	3	4
56. I would enjoy fast driving.	1	2	3	4
57. When I am very happy, I feel like it is ok to give in to cravings or overindulge.	1	2	3	4
58. Sometimes I do impulsive things that I later regret.	1	2	3	4
59. I am surprised at the things I do while in a great mood.	1	2	3	4

Scoring Instructions

This is a revised version of the UPPS Impulsive Behavior scale (Whiteside & Lynam, 2001). This version, UPPS-P (Lynam, Smith, Whiteside, & Cyders, 2006), assesses Positive Urgency (Cyders, Smith, Spillane, Fischer, Annus, & Peterson, 2007) in addition to the four pathways assessed in the original version of the scale-- Urgency (now Negative Urgency), (lack of) Premeditation, (lack of) Perseverance, and Sensation Seeking. The scale uses a 1 (agree strongly) to 4 (disagree strongly) response format. Because the items from different scales run in different directions, it is important to make sure that the correct items are reverse-scored. We suggest making all of the scales run in the direction such that higher scores indicate more impulsive behavior. Therefore, we include the scoring key for, (Negative) Urgency, (lack of) Premeditation, (lack of) Perseverance, Sensation Seeking, and Positive Urgency. For each scale, calculate the mean of the available items; this puts the scales on the same metric. We recommend requiring that a participant have at least 70% of the items before a score is calculated.

(Negative) Urgency (all items except 1 are reversed)
items 2 (R), 7(R), 12 (R), 17 (R), 22 (R), 29 (R), 34 (R), 39 (R), 44 (R), 50 (R), 53, 58 (R)

(lack of) Premeditation (no items are reversed)
items 1, 6, 11, 16, 21, 28, 33, 38, 43, 48, 55.

(lack of) Perseverance (two items are reversed)
items 4, 9 (R), 14, 19, 24, 27, 32, 37, 42, 47 (R)

Sensation Seeking (all items are reversed)
items 3 (R), 8 (R), 13 (R), 18 (R), 23 (R), 26 (R), 31 (R), 36 (R), 41 (R), 46 (R), 51 (R), 56 (R)

Positive Urgency (all items are reversed)
items 5 (R), 10 (R), 15 (R), 20 (R), 25 (R), 30 (R), 35 (R), 40 (R), 45 (R), 49 (R), 52 (R), 54 (R), 57 (R), 59 (R)

(R) indicates the item needs to be reverse scored such 1=4, 2=3, 3=2, and 4=1.